Nasal pneumococcal colonisation confers increased responsiveness to human alveolar macrophages against heterologous respiratory pathogens

Elena Mitsi[1,‡], Beatriz Carniel[1], Jesús Reiné[1], Jamie Rylance[1], Seher Zaidi[1], Alessandra Soares-Schanoski[2], Victoria Connor[1], Andrea Collins[1], Andreas Schlitzer[3], Elissavet Nikolaou[1], Carla Solórzano[1], Sherin Pojar[1], Helen Hill[1], Angela Hyder-Wright[1], Kondwani C. Jambo[4], Stephen B. Gordon[4], Simon P. Jochems[1,§] and Daniela M. Ferreira[1,§,‡]

[1]Department of Clinical Sciences, Liverpool School of Tropical Medicine, UK

[2]Bacteriology Laboratory, Butantan Institute. São Paulo, Brazil

[3]LIMES-Institute, University of Bonn, Germany

[4]Malawi Liverpool Wellcome Trust Clinical Research Programme, College of Medicine, P.O Box 30096, Chichiri, Blantyre, Malawi

§ joint senior authors

[‡]Correspondence: Elena Mitsi (elena.mitsi@lstmed.ac.uk), Daniela M. Ferreira (Daniela.ferreira@lstmed.ac.uk)

Department of Clinical Sciences, Liverpool School of Tropical Medicine, UK

SUMMARY

Pneumococcal pneumonia rates remain high globally, affecting the youngest and the oldest sections of the human population worldwide. Colonisation of the human nasopharynx is a pre-requisite for the development of both disease and immunity. How lung immunological memory to pneumococcus (*Spn*) is altered by colonisation of the nasopharynx is poorly described in humans. Traditionally, immunological memory is defined as T and B cell mediated, but more recently memory properties have been attributed to cells of innate immunity. We used a Controlled Human Infection Model to achieve nasal colonisation with 6B serotype and showed that aspirated pneumococci initiate a chain of reactions, leading to augmented, non-specific lung immunity. Alveolar macrophages increased their responsiveness to pneumococcus and other respiratory pathogen for three to four months after clearance of the nasal lumen from pneumococci. The local microenvironment facilitated monocytes differentiation and activation, shaping them phenotypically to AM cells. GM-CSF and IFN-γ elevated levels post carriage are likely to orchestrate the monocytes-to-macrophages differentiation and AMs activation. Active AMs had acquired M1-characteristics, as defined by function and gene expression. Our findings demonstrate that nasal pneumococcal carriage and micro-aspiration, trains pulmonary innate immune cells, leading to a brisker responsiveness to bacterial pathogens. The relative abundance of alveolar macrophages in the alveolar spaces, alongside with their long-life span and their potential for non-specific protection, make them an attractive target for novel vaccines.

INTRODUCTION

Streptococcus pneumoniae (the pneumococcus) is a leading cause of severe infectious diseases, responsible annually for the death of up to a million children worldwide(Liu et al., 2016). Pneumonia is the most frequent manifestation of pneumococcal disease (O'Brien et al., 2009) and despite the current vaccination strategies the burden of pneumococcal pneumonia remains very high globally (Wilson et al., 2017). Pneumonia affects disproportionally the very young and very old in both less and more developed countries (Bogaert et al., 2004). This susceptibility is attributed to an underdeveloped adaptive immune system in infants, and a waning acquired immunity combined with co-morbidities in the older adults (Franceschi et al., 2000).

Despite its pathogenicity, *S. pneumoniae* commonly colonises the human nasopharynx, a state known as pneumococcal colonisation or carriage (Bogaert et al., 2004). Pneumococcal carriage rates are at least 50% in infants and approximately 10-25% among adults (Goldblatt et al., 2005; Hussain et al., 2005). Exposure to pneumococcus through nasopharyngeal colonisation immunises the human body by eliciting both antibody and cellular immune-responses (Ferreira et al., 2013; McCool et al., 2002; Wright et al., 2013).

In contrast to nasal mucosal responses elicited by carriage (Ferreira et al., 2013; Mitsi et al., 2017), lung mucosal immune-responses to *Spn* are poorly described in humans. It is believed that protection against development of pneumonia relies on a successful regulation of colonisation in the nasopharynx and a brisk alveolar macrophage-mediated immune response in the lung (Jambo et al., 2010). The alveolar macrophage (AM) – an innate type resident lung cell- is an integral component of lung immunity and its long-lifespan aids function(Marriott and Dockrell, 2007). AMs are the first cells that combat pneumococci during early infection and the main cell population that mediates mucosal responses in the lower airways (Gordon and Read, 2002). They also play a key role in shaping adaptive immunity to a T helper 1 (Th1) or Th2 type response via cytokine secretion. Although AMs are mainly self-maintained, during

lung insult or as a result of ageing(Morales-Nebreda et al., 2015) their replenishment is contributed by peripheral monocytes in a macrophage colony-stimulating factor (M-CSF) and granulocyte macrophage (GM)-CSF-dependent manner (Guilliams et al., 2013; Hashimoto et al., 2013).

A clear understanding of the mechanisms that control brisk lung immune-responses at early stages of the infection, is essential to inform us why high rates of pneumonia persists in the high-risk groups (infants, elderly and immunocompromised), which are mainly characterized by underdeveloped or defective adaptive immunity. Although, current immunisation strategies to pneumococcal diseases target exclusively T and B-cell dependent immunity, the recently described memory properties of innate cells- natural killer (NK) cells and macrophages- indicated that innate immunity could be considered as a promising alternative or complementary vaccine target (Cheng et al., 2014; Netea et al., 2016; Quintin et al., 2014). In this study, we investigated the effect of pneumococcal carriage upon AMs- prototypical cells of innate lung immunity, on CD4+ T-cell responses, as well as the cross-talk between the AM-mediated innate and the adaptive lung immunity.

We showed for the first time that nasal human carriage, through pneumococcal aspiration, promotes monocytes differentiation, primes AMs and enhances their opsonophagocytic capacity against a range of bacterial respiratory pathogens. Interferon-γ (IFN-γ) responses were increased in the lung mucosa of pneumococcal (*Spn*) colonised individuals, whereas exogenous IFN-γ had a dose-dependent effect on AM function.

This immunological knowledge could have several implications for the development of more effective preventative strategies against pneumonia.

RESULTS

Alveolar macrophages exhibit augmented responsiveness to bacteria over three months after the clearance of nasal pneumococcal colonisation.

We used the experimental human pneumococcal carriage model (EHPC) and research bronchoscopy to investigate whether and how nasopharyngeal pneumococcal colonisation affects the lung immune responses. Bronchoalveolar lavage samples were collected from both pneumococcal (*Spn*) colonised and non-colonised healthy adults (aged from 18-50yrs) between one and seven months (29 to 203 days) post bacterial challenge (Figure 1a). Pneumococcal colonisation enhanced by 10% (± 12.9 SD) alveolar macrophage capacity to uptake pneumococci *in vitro* (p=0.005) (Figure1b). The differential AM opsonophagocytic activity (OPA) was robust and lasted for at least 4 months following the intranasal pneumococcal inoculation (Figure 1c). We also sought to examine whether this boosting effect was specific to pneumococcus or AM responses to other pathogens were similarly increased. AMs from *Spn* colonised individuals had greater capacity to uptake the respiratory pathogens *Streptococcus pyogenes* and *Staphylococcus aureus* when compared with AMs isolated from non-colonised individuals (p=0.009 and p=0.038 respectively, Figure 1d-f). Whilst we observed increased AMs responsiveness to gram-positive respiratory pathogens between the two groups, there was no significant difference in uptake of the gram-negative bacterium, *Escherichia coli* (Figure 1g).

CD4+ Th1 skewed responses rapidly prime AMs

To investigate whether the observed phenomenon was dependent on lung lymphocytes, we co-incubated AMs with autologous $CD3^{+}CD4^{+}$ T cells during *in vitro* infection with the challenged pneumococcal strain (*Spn6B*). The presence of $CD4^{+}$ T cells enhanced the basal AMs opsonophagocytic capacity in both non-colonised and *Spn* colonised individuals. Although, AMs uptake capacity differed between the two groups at baseline (prior to lung-derived autologous CD4+ addition), the presence of this cell subset further amplified the observed basal difference in AM pneumococcal uptake (Figure 2a). The increase in

pneumococcal uptake was 13.3% (±4.52 SD) and 23.4% (±5.84 SD), for non-colonised and *Spn* colonised respectively (Figure 2a).

To elucidate the mechanism underlying this increased boosting of AM function by $CD4^+$ T cells from *Spn* colonised individuals, we stained lung lymphocytes intracellularly for T-box transcription factor expressed in T-cells (T-bet), GATA-binding protein-3 (GATA-3) and Forkhead box P3 (Foxp3) transcription factors (Figure S1). In *Spn* colonised group the levels of $CD4^+$ T-bet expressing cells were twice as high than in non-colonised group ($p= 0.003$), indicating Th1-polarized responses. There was no significant difference in the levels of neither $CD4^+$ Gata-3 expressing nor $CD4^+$ Foxp3 expressing T cells between the two groups (Figure 2c-d), indicating lack of Treg responses.

In parallel, lymphocytes from both *Spn* colonised and non-colonised volunteers were stimulated with pneumococcal antigen (Heat Inactivated-*Spn6B*). Cytokine (IFN-γ, Tumour necrosis factor a [TNF-a] or Interleukin 17A [IL-17A]) producing $CD4^+$ T-cells were subsequently detected by flow cytometry (Figure S2). AMs OPA correlated with cytokine producing CD4+ T cells, classified as spontaneous (unstimulated) or pneumococcal-responding cells (Figure 3). Increased levels of IFN-γ producing $CD4^+$ T cells, both pneumococcal-specific and spontaneous responding, positively correlated with AMs ability to uptake live pneumococci *in vitro*. (Figure 3a). On the other hand, AMs OPA correlated positively with only the pneumococcal-specific TNF-a producing CD4+ T cells (Figure 3b), whereas IL-17A producing CD4+ T cells did not correlate with AMs OPA at any condition (Figure 3c).

Increased IFN-γ and GM-CSF levels are present in the alveolar spaces post nasal pneumococcal carriage

The alveolar microenvironment is crucial for cell signalling, shaping how local cells respond to different stimuli (Hussell and Bell, 2014). To assess alterations of the alveolar cytokine milieu

induced by nasal pneumococcal carriage, we measured levels of 30 cytokines and chemokines in the broncho-alveolar lavage (BAL) fluid retrieved from both *Spn* colonised and non-colonised individuals (Figure 4a, Table S1). Three cytokines had higher detectable levels in the BAL fluid of *Spn* colonised group: GM-CSF (p=0.03, Figure 4b) and pro-inflammatory cytokines IFN-γ (p=0.047, Figure 4c) and Interferon-α (IFN-α) (p=0.043, Figure 4d). To address the role of increased secretion of IFN-γ, a prototypic Th1 cytokine, in the pulmonary airspaces and its effect on AM function, we stimulated AMs with 10-fold increasing concentrations of exogenous IFN-γ. The lowest tested titers of IFN-γ (2 and 20ng/ml) augmented AMs OPA, resulting both in 30% increase in AM pneumococcal uptake (±3.26 and ±2.71 SD, respectively), whereas the highest used concentrations (200 and 2000ng/ml) failed to reach such an effect (Figure 4e). These results were verified when AM activation was assessed using a flow cytometric cytokine production assay (Figure 3). AMs produced increased levels of TNF-α in response to stimulation with HI-*Spn6B* at the same lower pre-stimulation doses of IFN-γ (Figure 4f). These data suggest that IFN-γ signalling is beneficial for AM function at lower doses, but not at higher concentration, with the mechanism to have a threshold which when exceeded can lead to AMs desensitisation**.**

Pneumococcal carriage reduces monocytes signature in the lung and alters alveolar macrophage gene expression.

Previously, we have demonstrated that AMs are not altered phenotypically by the presence of pneumococcus in the nasopharynx (Mitsi et al., 2018). However, given the increased capacity of AM to uptake pneumococcus, we further assessed the alterations that pneumococcal carriage confers to the lung myeloid cell lineage by immunophenotyping AMs and lung localised monocytes (Figure S4). *Spn*-colonised individuals displayed significantly greater AM levels (increased by 12.3% ± 4.33 SD) and higher AMs/monocytes ratio in the lung compared to non-colonised (Fig.5a). On the other hand, monocyte levels, both total and $CD14^{hi}CD16^{lo}$ and $CD14^{hi}CD16^{hi}$ subsets, had no significant difference between the two groups, despite their

trend for increased presence in the non-colonised group (Figure 5b-e). Similarly, no difference on neutrophils levels was observed between them (Figure 5b), indicating that nasal carriage in absence of disease does not lead to neutrophil recruitment to the lung.

To test whether pneumococcal colonisation led to monocyte differentiation, resulting in highly active AMs, we sought to identify the differential gene signatures of *Spn* colonised and non-colonised volunteers. We isolated AMs by cell sorting from a subset of BAL samples and performed NanoString expression analysis of 594 immunological genes. The analysis revealed 34 differentially expressed genes (DEG) between the two groups (Table S2). All genes, ranked from high to low expressed in the *Spn* colonised group, were enriched for pathways of cell differentiation and function, revealing under-presentation of monocytes surface markers and over-presentation of antigen-presentation markers in the *Spn* colonised group (Figure 5c). This further indicates that nasal carriage leads to monocyte-macrophage differentiation. When the AMs OPA per individual was compared with gene expression (log counts per million (CPM)- measured for each of the 594 genes, 34 genes were positively correlated with AMs function to uptake the bacteria (Table S3). Only four genes were both significantly correlated with AM OPA and significantly increased in *Spn* colonised individuals: ecto-5'-nucleotidase *(NT5E)* and T-box 21 (*TBX21)* (Figure 5d-e)*,* Carcinoembryonic antigen-related cell adhesion molecule 6 (*CEACAM6*) or CD66C and Toll like receptor 8 *(TLR8)* (not shown).

Pneumococcus can be detected in the lung after clearance of nasal colonisation

To investigate the mechanism that triggers the increased Th1 and AM responses in the pulmonary mucosa post nasal carriage, we sought to find evidence of the presence of the pneumococcal challenge strain in the alveolar spaces. For the detection of pneumococcus in the BAL samples, we utilised both molecular methods targeting a capsular polysaccharide gene specific to *Spn6B (wciP*- the rhamnosyl transferase gene) and classical microbiology. *Spn6B* DNA was detected in the BAL of 41% (9/22) of *Spn* colonised subjects (Table S4), 1

to 3 weeks following the clearance of nasal colonisation. Nasal pneumococcal density positively correlated with the copies of *Spn6B* DNA detected in BAL samples (Figure 6a). None of the non-colonised individuals had *Spn6B* DNA in their BAL sample. *Spn* colonised individuals differed in both density and duration of the carriage episode (Figure 6b). AMs capacity to uptake pneumococci correlated positively with nasal pneumococcal density (Figure 6c). Utilising confocal microscopy and anti-sera against the *Spn6B* capsule, we confirmed the relationship between nasal colonisation and presence of pneumococcal particles in the lung. Pneumococcal cells were found associated with the surface of AMs or internalised by them, a phenomenon only observed in the *Spn* colonised group (Figure 6d-e). These data suggest that during asymptomatic pneumococcal carriage pneumococcal aspiration occurs, and subsequently initiates pulmonary immunological responses.

DISCUSSION

This study provides insight into the immune responses elicited at the pulmonary mucosa during a colonisation episode of the nasopharynx. Here we have used an experimental human pneumococcal challenge (EHPC) model and bronchoscopic sampling in healthy volunteers post intranasal inoculation. We demonstrated that pneumococcal carriage, potentially through mechanic pneumococcal aspiration, leads to an enhanced and prolonged innate lung immunity, mediated by highly active AMs. The duration of the boosting effect exceeded the time of a seasonal period, lasting over three months post the clearance of colonisation.

The increased opsonophagocytic capacity displayed by AMs was a non-specific response to pneumococcal stimulus, as AMs responded with equal efficacy to both *Spn* and other gram-positive respiratory pathogens *in vitro*. By contrast, we did not see significant enhancement of AMs opsonophagocytic activity (OPA) against *E. coli.* Macrophages utilise different Toll-like receptors (TLRs) to recognise pathogens, which subsequently lead to differential activation of pathways. This could stand as one side of the explanation upon this observation. On the other

hand, the small sample size used might have limited the detection of a less pronounced difference between the two experimental groups.

Our overall observation resembles the findings of emerging studies on innate immune memory or 'trained immunity' (Cheng et al., 2014; Saeed et al., 2014), which emphasised the increased responsiveness of innate immune cells to microbial stimuli, caused by epigenetic changes post their activation by the stimulus (e.g. *Candida albicans* infection, Bacille Calmette-Guerin (BCG) or measles vaccination). Similarly to our observation, this augmented functional state persisted for weeks-to months, and moreover it conferred resistance to reinfection or heterologous infection (Kleinnijenhuis et al., 2012; Netea et al., 2016; Netea et al., 2011; Quintin et al., 2014).

The lung mucosa is not the sterile environment previously thought (Charlson et al., 2011; Man et al., 2017). The positive correlation between AMs OPA and nasal pneumococcal density suggested pneumococcal cell trafficking from the nasopharynx to the lung airways. By employing molecular, microbiology and visualisation methods, we demonstrated that pneumococcal aspiration occurs during nasal pneumococcal carriage, a phenomenon that was previously linked only to pneumonia cases (Albrich et al., 2012; Greenberg et al., 2011).

We have previously reported that carriage boosts pneumococcal-specific Th1 and Th17 cellular immunological memory in the human lung (Wright et al., 2013). Nevertheless, increased rates of pneumococcal carriage in children and clinical cases of pneumonia in adults have been associated with a reduction in systemic circulating Th-1 (IFN-γ secreting) $CD4^+$ T-cells (Kemp et al., 2002; Zhang et al., 2007). Polymorphisms in the adaptor MAL, which regulates IFN-γ signalling (Ni Cheallaigh et al., 2016), have been associated with altered susceptibility to a number of infectious diseases including severe pneumococcal disease (Khor et al., 2007). In HIV-infected adults, alveolar Th17 responses against *S. pneumoniae* are preserved (Peno et al., 2018), whereas the proportion of CD4+ T cells among lymphocytes is decreased, with loss of polyfunctional IFN-γ and TNF-α-secreting CD4+ cells (Jambo et al.,

2011), suggesting alternative mechanisms for their increased susceptible to pneumococcal pneumonia. Our findings on CD4+ Th1 skewed responses and exogenous IFN-γ effect on AM antimicrobial function support the idea that Th1 type responses and interferons are crucial in controlling bacteria at the early stages of infection. Moreover, we observed a rapid priming of AMs when co-cultured with autologous lung derived CD4+ T cells *in vitro*. Along the same lines, a very recent study in mice described a similar mechanistic link between adaptive and innate immune memory, suggesting that T cells can reciprocally interact with innate macrophages on the mucosal surface to prime them and trigger macrophage memory acquisition. T cells jump-started this process via IFN-γ (Yao et al., 2018).

In addition, our study highlighted that IFN-γ has dose-dependent effects on human AM function, which offers an explanation to the contradictory reports around this topic. For instance, in murine models high production of IFN-γ during influenza infection impaired phagocytosis and killing of *S. pneumoniae* by alveolar macrophages (Mina et al., 2015; Sun and Metzger, 2008). In contrast, many other evidences suggest that induction of IFN-γ secretion, related to non-acute viral infection, is beneficial for innate immune cells, promoting a range of antimicrobial functions, plus macrophages polarisation and activation (MacMicking, 2012; Matsuzawa et al., 2014; Yao et al., 2018).

Whereas the cytokine milieu in *Spn* colonised individuals, along with the CD4+ Th1 profile, suggest an AM polarisation towards the M1 phenotype, human AMs have been shown to co-express M1/M2 markers and therefore they do not fit neatly in the current macrophage classification (Hussell and Bell, 2014; Mitsi et al., 2018). Although, our knowledge on human AMs polarization states in homeostasis is largely unknown, a recent study highlighted that human AMs possess considerable phenotypic diversity (Morrell et al., 2018). By assessing AMs gene expression levels, we revealed that AM population derived from *Spn* colonised individuals was characterised by increased antigen-presentation and decreased monocytes signature. Our flow-based data corroborated this result by showing an increased AM to

monocyte ratio in colonised individuals. The positive correlation of AM OPA with genes such as *NT5E* (or CD73) (Eichin et al., 2015) and *TBX21* (a master regulator of Th1 responses) are indications that monocytes-to-macrophages differentiation and M1 polarisation occurs in the human lung in presence of carriage. Studies on human monocytes/macrophages have reported detectable expression of *CD73* in only M(LPS-TNF) polarised cells and increased of *T-bet* mRNA displayed by M1 polarised macrophages (Bachmann et al., 2012; Martinez et al., 2006). The positive association of AM OPA with TLR8 - an endosomal receptor that recognizes mainly single stranded RNA (ssRNA)- implies that viral ssRNA, such as influenza, might was present in the lung of a subset of individuals. Activation of TLR8 signalling pathways leads to production of proinflammatory cytokines and chemokines and to increased antiviral response. Whereas in this study we did not investigate the role of CD8+ T cells upon AM function, the late study conducted in mice revealed that effector CD8+ T cells, in the context of respiratory adenoviral infection, are able to prime AMs and render innate memory via IFN-γ production (Yao et al., 2018). Furthermore, it has been reported that activation of TLR8 signalling (TLR8-MyD88-IRAK4 signalling pathway) can reverse the suppression function of CD4+ Treg cells (Peng et al., 2005).

In addition, it would be of interest to investigate whether nasal colonisation leads to recruitment of monocytes to the alveolar spaces, as a response to partial depletion of AM resident population, which was not possible in the present study due to the single time point sampling. The one-time point sampling also disabled comparisons of immune-responses pre- and post-colonisation on an individual level. Therefore, future studies including baseline sampling of the lung mucosa will attribute clarity to the direct effect of *Spn* carriage on the pulmonary immune-responses.

In conclusion, this study emphasises the effect that nasal pneumococcal carriage has upon pulmonary immunity. The seeding of human lung with AM populations of different developmental origin, which exert prolonged, enhanced opsonophagocytic properties and

immunological memory, are findings with implications for vaccine development. Pneumococcal vaccines that focus solely on inducing a robust Th17 response may not be the best strategy for vaccine targeting serotype-independent protection against pneumonia. On the other hand, such a non-specific boosting of innate lung immunity, may be an alternative attractive strategy to successful pneumonia prevention, especially for the new-borns, whose immune system is still developing, or for the elderly, whose acquired immunity is beginning to wear off. In particular the elderly, who have been ascribed as the age group with the lowest pneumococcal colonisation rates and higher community acquired pneumonia cases, would benefit by the boosting effect that mucosal stimulation with whole cell pneumococcus confers to the pulmonary immunological mechanisms. These results suggest that a nasally administered live-attenuated pneumococcal vaccine could confer broad protection against pneumonia.

STAR METHODS

Study design and bronchoalveolar lavage collection

Healthy, non-smoking, adult volunteers aged from 18-50 years, enrolled in one of the Experimental Human Pneumococcal Carriage studies(Gritzfeld et al., 2013) between 2015-2018(Jochems et al., 2018; Jochems et al., 2017) underwent an one-off research bronchoscopy, as previously described(Mitsi et al., 2018; Zaidi et al., 2017). Experimental human pneumococcal challenge (EHPC) was conducted at Liverpool as previously described(Ferreira et al., 2013; Gritzfeld et al., 2013). Briefly, mid-log-growth vegitone culture of *Streptococcus pneumoniae* serotype 6B (strain BHN418) was prepared and stored at -80°C, and independently tested by Public Health England for purity and antibiotic sensitivity. 80,000 colony-forming-units (CFU) were sprayed into each nostril of participants. Pneumococcal colonisation was detected by classical microbiology methods and individuals were defined as Spn colonised (carriage positive) if any nasal wash culture following experimental challenge grew *S. pneumoniae* serotype 6B. Bronchoalveolar lavage samples were obtained from 29 to

203 days post intranasal pneumococcal inoculation (Fig.1a). *Spn* colonised (carriage positive) individuals received 3 doses of amoxicillin at the end of the clinical trial (at day 14, 27 or 29), prior to the bronchoscopy procedure.

Ethics statement

All volunteers gave written informed consent and research was conducted in compliance with all relevant ethical regulations. Ethical approval was given by the National Health Service Research Ethics Committee (REC). Ethics Committee reference numbers: 15/NW/0146, 14/NW/1460 and 15/NW/0931 and Human Tissue Authority licensing number: 12548.

Bacterial strains

S. pneumoniae strain 6B (BHN418) was cultured in Vegitone infusion broth (Fluka 41860, Sigma-Aldrich, Missouri, USA) for human intranasal inoculation or in Todd Hewitt broth supplemented with 0.5% yeast extract (THY) for the alveolar macrophage opsonophagocytic assay, at 37˚C with 5% CO_2 until early log phase. Similarly, *S. pyogenes* (MGA315) was cultured from a single colony in Brain Heart Infusion (BHI) broth overnight at 37ºC with 5% CO_2. *S. aureus (human isolate from EHPC trial)* and *E. coli* (NCTC86) were cultured in BHI and Luria Broth (LB), respectively, from a single colony overnight, on a shaking rotor at 37ºC with aeration. All bacterial stocks were grown till the early log phase and were stored at -80°C till further use.

Bronchoalveolar lavage processing

Bronchoalveolar lavages (BAL) samples were processed as previously described (Mitsi et al., 2018; Zaidi et al., 2017). Briefly, the BAL fluid was filtered using sterile gauze and centrifuged at 400g for 10 min at 4 °C. The supernatant was removed, the cell pellet was resuspended and washed with PBS. The centrifugation step was repeated once, and the cell pellet was resuspended in cold RPMI medium (Gibco™ RPMI 1640 Medium) containing antibiotics

(Penicillin, Neomycin and Streptomycin, Sigma-Aldrich, Sigma Chemical Co) (hereafter referred to as complete RPMI). Cell counts in each BAL sample were performed using a haemocytometer.

Alveolar macrophages isolation

AMs were routinely separated from other cell populations by seeding and adherence on 24-well plate (Greiner Bio-One, Kremsmünster, Austria), as previously described (Wright et al., 2012). After 4h adherence step, the non-adherent fraction was removed, and the AMs were washed with complete RPMI, following overnight incubation at 37˚C with 5% CO^2. In the experiments that highly pure AM population was requested, AMs were purified from the whole BAL sample through cell sorting (FACs ARIAII), following seeding on 96-well plate and overnight incubation at 37ºC, 5% CO^2.

Alveolar macrophage opsonophagocytic killing (OPA)

AMs opsonophagocytic capacity was evaluated as previously described with minor modifications (Wright et al., 2013). Briefly, live *S. pneumoniae* serotype 6B (inoculation strain) or *S. pyogenes* or *S. aureus* or *E. coli* were opsonized in a 1:16 final dilution of human intravenous immunoglobulin (IVIG, Gamunex, Grifols Inc, Spain) in HBSS $^{+/+}$ (with Ca^{2+} Mg^{2+}) at 37ºC for 15min. AMs were washed twice with RPMI without antibiotics, and incubated with an opsonized bacterial strain in Opsonisation Buffer B (HBSS $^{+/+}$ plus 1% gelatine solution and 5% FBS) and baby rabbit complement (Mast Group) at 37˚C on a shaking rotor for 60min. Multiplicity of infection (MOI) used was 1 :100 for all the gram-positive bacteria. Opsonophagocytic killing assay for the gram-negative (*E. coli*) was modified as described elsewhere (MOI= 1:20 for 30min)(Abbanat et al., 2017). In the assays where isolated by cell sorting AMs were infected with opsonised *spn6B*, the MOI was modified to 1:20 due to increased loss of cells during the high-throughput cell sorting. In some experiments AMs were stimulated with 2ng/ml, 20ng/ml, 200ng/ml and 2,000ng/ml of recombinant IFN-γ (Bio-techne).

Flow cytometry assays

In each flow cytometry assays, the corresponding cell population was stained with predetermined optimal concentration of fluorochrome-conjugated monoclonal antibodies against human cell surface proteins or intracellular cytokines.

AM and monocyte immunophenotyping: Myeloid lineage cells were immunophenotyped using monoclonal antibodies for key surface markers. In brief, whole BAL cells (1 x 10^6 cells) were stained with Aqua Viability dye (LIVE/DEAD® Fixable Dead Cell Stain kit, Invitrogen, UK), anti-CD45 FITC, anti-CD80 APC-H7, anti-CD86 PE, anti-CD206 PE-CF594, anti-CD14 PerCP Cy5.5, anti-CD16 PE Cy7, anti-CD163 APC, anti-CD11b AF700, anti-CD11C PB, anti-CD64 BV605 and anti-HLADR BV785. All the samples were acquired on a FacsAria III sorter/cytometer (BD Biosciences) and analyzed using Flowjo version 10 (Treestar). BAL samples with macroscopically visual red blood cell contamination were excluded from the analysis.

AM stimulation with HI-Spn6B and IFN-γ: 1 million of BAL cells per condition, resuspended in complete RPMI, were added in 24-well plate and incubated overnight at 37ºC, 5% CO_2. Non-adherent cells were removed, and AMs were washed 3x with pre-warmed plain RPMI, following stimulation with 10x increased concentration of IFN-γ (2ng/ml, 20ng/ml, 200ng/ml and 2,000ng/ml) for 30min. Post the cytokines stimulation, cells received 5µg/ml of heat-inactivated (HI) Spn6B and were incubated for 2 hours. Non-cytokine/non-*Spn* treated and non-cytokine/*Spn* treated controls were included per volunteer. Cytokines were retained within the cells by the addition of GolgiPlug (BD Biosciences) and stimulation for 2 more hours. Post incubation time, AMs were washed with PBS and detached from the wells by adding of 2.5mM EDTA solution. Cells were collected in FACs tubes and pelleted (1500 rpm for 10 min centrifugation), following staining for human AM surface markers - anti-CD14 PerCyP5.5, anti-CD169-PE, CD206 PE-CF594 and CD45- Pacific Orange- and anti-TNF-a BV605 (BD Biosciences).

Transcription factors analysis: 1 million of BAL cells were washed with 3 mL of PBS and stained with Aqua Viability dye (LIVE/DEAD Fixable Dead Cell Stain kit, Invitrogen, UK) and the surface markers CD3-APC.cy7, CD4–PerCP5.5, CD8–AF700, CD69–BV650, CD49a-APC, anti-CD25-PE.TexasRed and CD45-BV711 (Biolegend, San Diego, CA). For permeabilization and fixation, Foxp3/Transcription Factor Staining Buffer Set (eBiosciences, San Diego, CA) was used as per the manufacturer's instructions, following intracellular staining with T-bet-APC, Gata-3-PE and Foxp3-FITC. All samples were acquired on a LSRII flow cytometer (BD Biosciences).

INF-γ, TNF-a and IL-17 producing CD4+ T cells post stimulation with HI-Spn6B: Cells were harvested, stained and analysed as previously described, with minor modifications(Wright et al., 2013; Wright et al., 2012). In brief, non-adherent cells were collected from the BAL samples post an adherence step, centrifuged at 1,500rpm for 5min, resuspended in complete RPMI and seeded in 96-well plates at equal concentrations of 600,000 to 1 million cells per condition. Cells were stimulated with 5µg/ml of HI-Spn6B and incubated for 2 hours at 37ºC, following addition of GolgiPlug (BD Biosciences) and overnight incubation at 37ºC, 5% CO_2. A non-stimulated with Spn6B (mock) cell condition was included per volunteer. After 16 hours, the cells were washed with PBS and stained with Violet Viability dye (LIVE/DEAD Fixable Dead Cell Stain kit, Invitrogen, UK) and anti-CD3-APCH7, TCR-γδ–PECy7 (BD Biosciences, USA), anti-CD4–PerCP5.5, anti-CD8–AF700, anti-CD69–BV650, anti-CD25-PE.TxsRed, anti-CD103–BV605, anti-CD49a-APC (Biolegend, San Diego, CA). For the assessment of intracellular cytokine production, after permeabilization and fixation, the cells were stained with the following markers: anti-IFN-γ-PE, anti-IL17A–BV510 and TNF-α–BV711 (BD Biosciences). All samples were acquired on a LSRII flow cytometer (BD Biosciences).

Luminex analysis of Bronchoalveolar lavage fluid

The acellular BAL fluid (BAL supernatant) was collected post centrifugation of whole BAL sample (400g for 10min at 4ºC), divided to 1ml aliquots and stored at -80ºC until analysis. On

the day of the analysis samples were concentrated x10 (1ml of BAL concentrated to 100ul using vacuum concentrator RVC2-18), following acquisition using a 30-plex magnetic Luminex cytokine kit (ThermoFisher) and analysed on a LX200 with xPonent3.1 software following manufacturer's instructions. Samples were analysed in duplicates and BAL samples with a CV > 50 % were excluded.

AMs gene analysis using Nanostring platform

Nanostring was used as previously described(Jochems et al., 2018). Briefly, AMs were sorted by FACsARIA II cell sorter and stored in RLT buffer (Qiagen) with 1% 2-mercaptoethanol (Sigma) at -80C until RNA extraction. Extraction was performed using the RNEasy micro kit (Qiagen) with on column DNA digestion. Extracted RNA was quantified by qPCR targeting B2M gene (Bioanalyzer, Agilent). The single cell immunology v2 kit (Nanostring) was used with 20 pre-amp cycles for all samples. Hybridized samples were prepared on a Prep Station and scanned on a nCounter® MAX (Nanostring). Raw counts were analysed using the R/Bioconductor package DESeq2 for internal normalization, which gave lower variance than normalizing to included housekeeping genes. DEG were identified using a model matrix correcting for repeated individual measurements. Log CPM from raw counts were calculated using the 'edgeR' package. 2logFold chances were further analysed by the 'fgsea' package, through BMT pathways gene set enrichment analysis.

Bacterial DNA extraction from BAL samples

Extraction of bacterial DNA from the BAL samples was performed as previously described with minor modifications (VC,2018, EN,2018 or EG,2018). Briefly, 15mls of BAL sample was centrifuged at 4,000rpm for 15min. Following centrifugation, the supernatant was discarded, and DNA was extracted from the pellet using the Agowa kit for bacterial DNA extraction. The extracted DNA was eluted in a volume of 63ul of elution buffer. DNA purity and quality were assessed by a spectrophotometer (Nanodrop ND-1000, Thermo Fisher Scientific).

Quantification of pneumococcal DNA by qPCR

Presence of pneumococcal DNA in BAL samples was determined using primers and probe specifically designed for 6B serotype, targeting on a capsular polysaccharide gene known as *wciP*, the rhamnosyl transferase gene. The primers and probe sequences were: forward primer 5'- GCTAGAGATGGTTCCTTCAGTTGAT- 3'; reverse primer 5'- CATACTCTAGTGCAAACTTTGCAAAAT- 3' and probe 5'- [FAM] ACT GTC TCA TGA TAA TT [MGBEQ] -3' as previously published (Tarrago et al., 2008). Primers and probe used in their optimised concentrations, 900nM primers and 200nM TaqMan MGB probe per reaction. A non-template control and a negative control per DNA extraction, were included in every run. DNA was amplified with the real-time PCR System (Agilent Technologies, Statagene Mx3005P) by using the following cycling parameters: 95°C for 10 min, followed by 40 cycles at 95°C for 15 sec and 60°C for 1 min. A standard curve of a 10-fold dilution series of genomic DNA extracted from SPN6B was used. The genomic DNA was extracted using the Qiagen Genomic-tip 20/G Kit (Qiagen) and quantified by nanodrop. The conversion from weight pneumococcal DNA to number of DNA copies *S. pneumoniae* was based on the weight of one genome copy TIGR4 calculated by the genome length in base pairs times the weight of a DNA base pair (650 Dalton). The lower limit of detection (LLOD) of the method was set at 40 cycles. Amplification values >40. A sample was considered positive if at least two of three yielded a positive result within the <40-cycle cut-off. Data was analysing using MxPro software.

Confocal microscopy

Fresh BAL cells were washed and stained for surface markers (anti-CD14 texas Red and CD45-AlexaFluor647). Cells were permeabilised and incubated with anti-6B pneumococcal antisera for 30 minutes on ice and then secondary-conjugated antibody (anti-rabbit 488) for 30 more minutes. After washing, cells were cytospun onto microscope slides and allowed to air dry. DAPI solution was applied directly on the spun cells for 5 minutes. After washing, samples were mounted using Aqua PolyMount (VWR International) with a coverslip onto the

microslide. The entire cytospin for each sample was manually viewed by microscopy for detection of pneumococci. Multiple fields of view (>3) were imaged for each sample. Images were captured using either an inverted TissueFAXS Zeiss Confocal Microscope. Z stacks were recorded at 1μm intervals at either 40x oil or 63x oil objectives. The confocal microscope operator (CW) was blinded to the colonisation status of the volunteer at the time of sampling.

Quantification and statistical analysis

Statistical analyses were performed using GraphPad Prism (Version 6, GraphPad Software, La Jolla, CA) and R software (version 3.5.1), including Bioconductor packages. Two-tailed statistical tests were used throughout the study. If two parametric groups were compared, a two-tailed t test was used for unpaired and paired groups. If two non-parametric groups were compared, a Mann-Whitney or Wilcoxon test was used for unpaired and paired groups respectively. When log-normalized data was not normally distributed, non-parametric tests were performed. For gene expression and Luminex analysis p values were corrected by applying multiple correction testing (Benjamin-Hochberg). To quantify association between groups, Pearson or Spearman correlation test was used for parametric or non-parametric groups, respectively. Differences were considered significant at $p \leq 0.05$ (*$p< 0.05$, **$p< 0.01$, ***$p< 0.001$, ****$p< 0.0001$).

ACKNOWLEDGMENTS

We would like to thank all the subjects who participated in this study, as well as all staff of the Clinical Research Unit at the Royal Liverpool Hospital and the clinical staff of the Respiratory Infection Group at the Liverpool School of Tropical Medicine. We also thank Dr. Caroline Weight for operating the confocal microscope and Dr. Robert Adams for providing the E. coli strain (NCTC86). This work was funded by the Bill and Melinda Gates Foundation

(OPP1117728) and the Medical Research Council (MR/K01188X/1) grants awarded to D.M.F and S.B.G. Flow cytometric acquisition was performed on a BD LSRII and cell sorting on a BD FACs ARIA funded by Wellcome Trust Multi-User Equipment grant (104936/Z/14/Z). S.P.J received support from Royal Society of Tropical Medicine and Hygiene for NanoString analysis.

DISCLOSURE

The authors have no conflict of interest to declare.

REFERENCES

Abbanat, D., Davies, T.A., Amsler, K., He, W., Fae, K., Janssen, S., Poolman, J.T., and van den Dobbelsteen, G. (2017). Development and Qualification of an Opsonophagocytic Killing Assay To Assess Immunogenicity of a Bioconjugated Escherichia coli Vaccine. Clin Vaccine Immunol *24*.

Albrich, W.C., Madhi, S.A., Adrian, P.V., van Niekerk, N., Mareletsi, T., Cutland, C., Wong, M., Khoosal, M., Karstaedt, A., Zhao, P.*, et al.* (2012). Use of a rapid test of pneumococcal colonization density to diagnose pneumococcal pneumonia. Clin Infect Dis *54*, 601-609.

Bachmann, M., Scheiermann, P., Hardle, L., Pfeilschifter, J., and Muhl, H. (2012). IL-36gamma/IL-1F9, an innate T-bet target in myeloid cells. J Biol Chem *287*, 41684-41696.

Bogaert, D., De Groot, R., and Hermans, P.W. (2004). Streptococcus pneumoniae colonisation: the key to pneumococcal disease. Lancet Infect Dis *4*, 144-154.

Charlson, E.S., Bittinger, K., Haas, A.R., Fitzgerald, A.S., Frank, I., Yadav, A., Bushman, F.D., and Collman, R.G. (2011). Topographical continuity of bacterial populations in the healthy human respiratory tract. Am J Respir Crit Care Med *184*, 957-963.

Cheng, S.C., Quintin, J., Cramer, R.A., Shepardson, K.M., Saeed, S., Kumar, V., Giamarellos-Bourboulis, E.J., Martens, J.H., Rao, N.A., Aghajanirefah, A.*, et al.* (2014). mTOR- and HIF-1alpha-mediated aerobic glycolysis as metabolic basis for trained immunity. Science *345*, 1250684.

Eichin, D., Laurila, J.P., Jalkanen, S., and Salmi, M. (2015). CD73 Activity is Dispensable for the Polarization of M2 Macrophages. PLoS One *10*, e0134721.

Ferreira, D.M., Neill, D.R., Bangert, M., Gritzfeld, J.F., Green, N., Wright, A.K., Pennington, S.H., Bricio-Moreno, L., Moreno, A.T., Miyaji, E.N.*, et al.* (2013). Controlled human infection and rechallenge with Streptococcus pneumoniae reveals the protective efficacy of carriage in healthy adults. Am J Respir Crit Care Med *187*, 855-864.

Franceschi, C., Bonafe, M., and Valensin, S. (2000). Human immunosenescence: the prevailing of innate immunity, the failing of clonotypic immunity, and the filling of immunological space. Vaccine *18*, 1717-1720.

Goldblatt, D., Hussain, M., Andrews, N., Ashton, L., Virta, C., Melegaro, A., Pebody, R., George, R., Soininen, A., Edmunds, J.*, et al.* (2005). Antibody responses to nasopharyngeal carriage of Streptococcus pneumoniae in adults: a longitudinal household study. J Infect Dis *192*, 387-393.

Gordon, S.B., and Read, R.C. (2002). Macrophage defences against respiratory tract infections. Br Med Bull *61*, 45-61.

539 Greenberg, D., Givon-Lavi, N., Newman, N., Bar-Ziv, J., and Dagan, R. (2011). Nasopharyngeal carriage
540 of individual Streptococcus pneumoniae serotypes during pediatric pneumonia as a means to estimate
541 serotype disease potential. Pediatr Infect Dis J *30*, 227-233.
542 Gritzfeld, J.F., Wright, A.D., Collins, A.M., Pennington, S.H., Wright, A.K., Kadioglu, A., Ferreira, D.M.,
543 and Gordon, S.B. (2013). Experimental human pneumococcal carriage. J Vis Exp.
544 Guilliams, M., De Kleer, I., Henri, S., Post, S., Vanhoutte, L., De Prijck, S., Deswarte, K., Malissen, B.,
545 Hammad, H., and Lambrecht, B.N. (2013). Alveolar macrophages develop from fetal monocytes that
546 differentiate into long-lived cells in the first week of life via GM-CSF. J Exp Med *210*, 1977-1992.
547 Hashimoto, D., Chow, A., Noizat, C., Teo, P., Beasley, M.B., Leboeuf, M., Becker, C.D., See, P., Price, J.,
548 Lucas, D.*, et al.* (2013). Tissue-resident macrophages self-maintain locally throughout adult life with
549 minimal contribution from circulating monocytes. Immunity *38*, 792-804.
550 Hussain, M., Melegaro, A., Pebody, R.G., George, R., Edmunds, W.J., Talukdar, R., Martin, S.A.,
551 Efstratiou, A., and Miller, E. (2005). A longitudinal household study of Streptococcus pneumoniae
552 nasopharyngeal carriage in a UK setting. Epidemiol Infect *133*, 891-898.
553 Hussell, T., and Bell, T.J. (2014). Alveolar macrophages: plasticity in a tissue-specific context. Nat Rev
554 Immunol *14*, 81-93.
555 Jambo, K.C., Sepako, E., Fullerton, D.G., Mzinza, D., Glennie, S., Wright, A.K., Heyderman, R.S., and
556 Gordon, S.B. (2011). Bronchoalveolar CD4+ T cell responses to respiratory antigens are impaired in
557 HIV-infected adults. Thorax *66*, 375-382.
558 Jambo, K.C., Sepako, E., Heyderman, R.S., and Gordon, S.B. (2010). Potential role for mucosally active
559 vaccines against pneumococcal pneumonia. Trends Microbiol *18*, 81-89.
560 Jochems, S.P., Marcon, F., Carniel, B.F., Holloway, M., Mitsi, E., Smith, E., Gritzfeld, J.F., Solorzano, C.,
561 Reine, J., Pojar, S.*, et al.* (2018). Inflammation induced by influenza virus impairs human innate
562 immune control of pneumococcus. Nat Immunol *19*, 1299-1308.
563 Jochems, S.P., Piddock, K., Rylance, J., Adler, H., Carniel, B.F., Collins, A., Gritzfeld, J.F., Hancock, C.,
564 Hill, H., Reine, J.*, et al.* (2017). Novel Analysis of Immune Cells from Nasal Microbiopsy Demonstrates
565 Reliable, Reproducible Data for Immune Populations, and Superior Cytokine Detection Compared to
566 Nasal Wash. PLoS One *12*, e0169805.
567 Kemp, K., Bruunsgaard, H., Skinhoj, P., and Klarlund Pedersen, B. (2002). Pneumococcal infections in
568 humans are associated with increased apoptosis and trafficking of type 1 cytokine-producing T cells.
569 Infect Immun *70*, 5019-5025.
570 Khor, C.C., Chapman, S.J., Vannberg, F.O., Dunne, A., Murphy, C., Ling, E.Y., Frodsham, A.J., Walley,
571 A.J., Kyrieleis, O., Khan, A.*, et al.* (2007). A Mal functional variant is associated with protection against
572 invasive pneumococcal disease, bacteremia, malaria and tuberculosis. Nat Genet *39*, 523-528.
573 Kleinnijenhuis, J., Quintin, J., Preijers, F., Joosten, L.A., Ifrim, D.C., Saeed, S., Jacobs, C., van Loenhout,
574 J., de Jong, D., Stunnenberg, H.G.*, et al.* (2012). Bacille Calmette-Guerin induces NOD2-dependent
575 nonspecific protection from reinfection via epigenetic reprogramming of monocytes. Proc Natl Acad
576 Sci U S A *109*, 17537-17542.
577 Liu, L., Oza, S., Hogan, D., Chu, Y., Perin, J., Zhu, J., Lawn, J.E., Cousens, S., Mathers, C., and Black, R.E.
578 (2016). Global, regional, and national causes of under-5 mortality in 2000-15: an updated systematic
579 analysis with implications for the Sustainable Development Goals. Lancet *388*, 3027-3035.
580 MacMicking, J.D. (2012). Interferon-inducible effector mechanisms in cell-autonomous immunity. Nat
581 Rev Immunol *12*, 367-382.
582 Man, W.H., de Steenhuijsen Piters, W.A., and Bogaert, D. (2017). The microbiota of the respiratory
583 tract: gatekeeper to respiratory health. Nat Rev Microbiol *15*, 259-270.
584 Marriott, H.M., and Dockrell, D.H. (2007). The role of the macrophage in lung disease mediated by
585 bacteria. Exp Lung Res *33*, 493-505.
586 Martinez, F.O., Gordon, S., Locati, M., and Mantovani, A. (2006). Transcriptional profiling of the human
587 monocyte-to-macrophage differentiation and polarization: new molecules and patterns of gene
588 expression. J Immunol *177*, 7303-7311.

589 Matsuzawa, T., Fujiwara, E., and Washi, Y. (2014). Autophagy activation by interferon-gamma via the
590 p38 mitogen-activated protein kinase signalling pathway is involved in macrophage bactericidal
591 activity. Immunology *141*, 61-69.
592 McCool, T.L., Cate, T.R., Moy, G., and Weiser, J.N. (2002). The immune response to pneumococcal
593 proteins during experimental human carriage. J Exp Med *195*, 359-365.
594 Mina, M.J., Brown, L.A., and Klugman, K.P. (2015). Dynamics of Increasing IFN-gamma Exposure on
595 Murine MH-S Cell-Line Alveolar Macrophage Phagocytosis of Streptococcus pneumoniae. J Interferon
596 Cytokine Res *35*, 474-479.
597 Mitsi, E., Kamng'ona, R., Rylance, J., Solorzano, C., Jesus Reine, J., Mwandumba, H.C., Ferreira, D.M.,
598 and Jambo, K.C. (2018). Human alveolar macrophages predominately express combined classical M1
599 and M2 surface markers in steady state. Respir Res *19*, 66.
600 Mitsi, E., Roche, A.M., Reine, J., Zangari, T., Owugha, J.T., Pennington, S.H., Gritzfeld, J.F., Wright, A.D.,
601 Collins, A.M., van Selm, S.*, et al.* (2017). Agglutination by anti-capsular polysaccharide antibody is
602 associated with protection against experimental human pneumococcal carriage. Mucosal Immunol
603 *10*, 385-394.
604 Morales-Nebreda, L., Misharin, A.V., Perlman, H., and Budinger, G.R. (2015). The heterogeneity of lung
605 macrophages in the susceptibility to disease. Eur Respir Rev *24*, 505-509.
606 Morrell, E.D., Wiedeman, A., Long, S.A., Gharib, S.A., West, T.E., Skerrett, S.J., Wurfel, M.M., and
607 Mikacenic, C. (2018). Cytometry TOF identifies alveolar macrophage subtypes in acute respiratory
608 distress syndrome. JCI Insight *3*.
609 Netea, M.G., Joosten, L.A., Latz, E., Mills, K.H., Natoli, G., Stunnenberg, H.G., O'Neill, L.A., and Xavier,
610 R.J. (2016). Trained immunity: A program of innate immune memory in health and disease. Science
611 *352*, aaf1098.
612 Netea, M.G., Quintin, J., and van der Meer, J.W. (2011). Trained immunity: a memory for innate host
613 defense. Cell Host Microbe *9*, 355-361.
614 Ni Cheallaigh, C., Sheedy, F.J., Harris, J., Munoz-Wolf, N., Lee, J., West, K., McDermott, E.P., Smyth, A.,
615 Gleeson, L.E., Coleman, M.*, et al.* (2016). A Common Variant in the Adaptor Mal Regulates Interferon
616 Gamma Signaling. Immunity *44*, 368-379.
617 O'Brien, K.L., Wolfson, L.J., Watt, J.P., Henkle, E., Deloria-Knoll, M., McCall, N., Lee, E., Mulholland, K.,
618 Levine, O.S., Cherian, T.*, et al.* (2009). Burden of disease caused by Streptococcus pneumoniae in
619 children younger than 5 years: global estimates. Lancet *374*, 893-902.
620 Peng, G., Guo, Z., Kiniwa, Y., Voo, K.S., Peng, W., Fu, T., Wang, D.Y., Li, Y., Wang, H.Y., and Wang, R.F.
621 (2005). Toll-like receptor 8-mediated reversal of CD4+ regulatory T cell function. Science *309*, 1380-
622 1384.
623 Peno, C., Banda, D.H., Jambo, N., Kankwatira, A.M., Malamba, R.D., Allain, T.J., Ferreira, D.M.,
624 Heyderman, R.S., Russell, D.G., Mwandumba, H.C.*, et al.* (2018). Alveolar T-helper 17 responses to
625 streptococcus pneumoniae are preserved in ART-untreated and treated HIV-infected Malawian adults.
626 J Infect *76*, 168-176.
627 Quintin, J., Cheng, S.C., van der Meer, J.W., and Netea, M.G. (2014). Innate immune memory: towards
628 a better understanding of host defense mechanisms. Curr Opin Immunol *29*, 1-7.
629 Saeed, S., Quintin, J., Kerstens, H.H., Rao, N.A., Aghajanirefah, A., Matarese, F., Cheng, S.C., Ratter, J.,
630 Berentsen, K., van der Ent, M.A.*, et al.* (2014). Epigenetic programming of monocyte-to-macrophage
631 differentiation and trained innate immunity. Science *345*, 1251086.
632 Sun, K., and Metzger, D.W. (2008). Inhibition of pulmonary antibacterial defense by interferon-gamma
633 during recovery from influenza infection. Nat Med *14*, 558-564.
634 Tarrago, D., Fenoll, A., Sanchez-Tatay, D., Arroyo, L.A., Munoz-Almagro, C., Esteva, C., Hausdorff, W.P.,
635 Casal, J., and Obando, I. (2008). Identification of pneumococcal serotypes from culture-negative
636 clinical specimens by novel real-time PCR. Clin Microbiol Infect *14*, 828-834.
637 Wilson, R., Cohen, J.M., Reglinski, M., Jose, R.J., Chan, W.Y., Marshall, H., de Vogel, C., Gordon, S.,
638 Goldblatt, D., Petersen, F.C.*, et al.* (2017). Naturally Acquired Human Immunity to Pneumococcus Is
639 Dependent on Antibody to Protein Antigens. PLoS Pathog *13*, e1006137.

640 Wright, A.K., Bangert, M., Gritzfeld, J.F., Ferreira, D.M., Jambo, K.C., Wright, A.D., Collins, A.M., and
641 Gordon, S.B. (2013). Experimental human pneumococcal carriage augments IL-17A-dependent T-cell
642 defence of the lung. PLoS Pathog *9*, e1003274.
643 Wright, A.K., Ferreira, D.M., Gritzfeld, J.F., Wright, A.D., Armitage, K., Jambo, K.C., Bate, E., El Batrawy,
644 S., Collins, A., and Gordon, S.B. (2012). Human nasal challenge with Streptococcus pneumoniae is
645 immunising in the absence of carriage. PLoS Pathog *8*, e1002622.
646 Yao, Y., Jeyanathan, M., Haddadi, S., Barra, N.G., Vaseghi-Shanjani, M., Damjanovic, D., Lai, R.,
647 Afkhami, S., Chen, Y., Dvorkin-Gheva, A.*, et al.* (2018). Induction of Autonomous Memory Alveolar
648 Macrophages Requires T Cell Help and Is Critical to Trained Immunity. Cell.
649 Zaidi, S.R., Collins, A.M., Mitsi, E., Reine, J., Davies, K., Wright, A.D., Owugha, J., Fitzgerald, R., Ganguli,
650 A., Gordon, S.B.*, et al.* (2017). Single use and conventional bronchoscopes for Broncho alveolar lavage
651 (BAL) in research: a comparative study (NCT 02515591). BMC Pulm Med *17*, 83.
652 Zhang, Q., Bagrade, L., Bernatoniene, J., Clarke, E., Paton, J.C., Mitchell, T.J., Nunez, D.A., and Finn, A.
653 (2007). Low CD4 T cell immunity to pneumolysin is associated with nasopharyngeal carriage of
654 pneumococci in children. J Infect Dis *195*, 1194-1202.

655

656

657 **Figure Legends**

658

659 **Figure 1: AMs display an increased opsonophagocytic activity (OPA) against bacterial pathogens for**
660 **a prolonged period post nasal pneumococcal carriage. a)** Defined time period of BAL samples
661 collection from *Spn* colonised and non- colonised individuals within three independent Experimental
662 Human Pneumococcal Challenge (EHPC) studies. **b)** Capacity of AMs derived from non-colonised
663 individuals (Carriage neg - black dots, n= 35) and *Spn* colonised individuals (Carriage pos - red circles,
664 n=36) to uptake pneumococci *in vitro* (p=0.005) by Mann-Whitney test. Geometric mean with 95% CI.
665 Multiplicity of infection (MOI) used was 1: 100. **c)** Chronological representation of all BAL samples
666 (n=71) collected from one to six months post intranasal pneumococcal inoculation divided into three
667 consecutive time periods. T1: p= 0.001, T2: p= 0.003 and T3: p= 0.82 by Mann-Whitney test. Geometric
668 mean with 95% CI. **d-g)** AMs capacity to uptake *Spn6B*, *S. aureus, S. pyogenes* and *E. coli*. Geometric
669 mean with 95% CI. **p= 0.009, *p= 0.038, **p= 0.009 and p=0.25 by Mann-Whitney test.

670

671 **Figure 2: AMs priming and cross-talk with autologous CD4+ T subsets. a)** Comparison of phagocytic
672 activity between sorted AM and sorted AM plus autologous BAL isolated $CD4^+$ T cells from both *Spn*
673 colonised (n= 13) and non-colonised individuals (n=11). MOI=1:20. AM and $CD4^+$ T cells were used in
674 a 10:1 ratio. p< 0.0001 in both groups by paired t-test. Comparison of AM basal killing activity between
675 the two groups. *p= 0.018 by unpaired t-test with Welch's correction. Comparison of AM killing
676 activity in the presence of lung CD4+ T cells between carriage negative and positive volunteers. **p=
677 0.001 by unpaired t-test with Welch's corrections. **b-d)** Intracellular staining of $CD4^+$ T cells for T-bet,
678 Gata-3 and Foxp3 transcription factors as percentage of $CD3^+CD4^+$ BAL lymphocytes. Geometric mean
679 with 95% CI. **p= 0.003, p= 0.85, p= 0.33 respectively by unpaired t-test with Welch correction test.

680

681 **Figure 3: Associations of AM phagocytic activity with CD4+ Th1 and Th17 responses. a)** From left to
682 right are illustrated correlations between levels of IFN-γ expressing CD4+ T cells at baseline (non-
683 stimulated), total IFN-γ expressing CD4+ T cells post stimulation with Heat Inactivated (HI) *Spn6B* and
684 the *Spn*-specific responding CD4+ T cells (unstimulated condition subtracted from *Spn*-stimulated
685 condition) with alveolar macrophage OPA. Spearman Rho and p values are shown. **b)** Correlation of
686 *Spn*-specific, TNF-a expressing CD4+ T cells with AM OPA. Spearman Rho and p value are shown. **c)**
687 From left to right are illustrated the levels of IL-17A expressing CD4+ T cells at baseline and the levels
688 of total and Spn-specific, IL-17A expressing CD4+ T cells in association with AM OPA. No significant
689 correlations. Spearman Rho and p values are shown.

690 **Figure 4: Lung cytokine milieu, alterations post nasal carriage and the effect of IFN-γ on AMs**
691 **opsonophagocytic function.**
692 **a)** Heatmap of the 30 cytokines levels, expressed as log10 median (pg/mL), measured in the BAL fluid
693 (n=20 carriage negative and n=22 carriage positive individuals). **b-d)** Levels of significantly different
694 cytokines between the two groups, expressed as pg/ml. GM-CSF, IFN-γ and IFN-a with *p= 0.032,
695 *p=0.047 and *p=0.043 respectively, analysed by Mann-Whitney test. **e)** The effect of 10x increasing
696 doses of exogenous IFN-γ (2-2000ng/ml) on the capacity of AM to uptake pneumococcus (live Spn6B
697 used, MOI= 1:100) . AM isolated from 6 non-challenged subjects. Individuals samples are depicted and
698 connected with dashed lines. ** p< 0.01 by Friedman test followed by Dunn's multiple comparison. **f)**
699 TNF-a production from AMs, pre-treated or not with exogenous IFN-γ (2-2000ng/ml), following
700 stimulation with HI-*Spn6B*. AM isolated from 4 non-challenged subjects. Individuals samples are
701 depicted and connected with dashed lines. *p< 0.05, ** p< 0.01 by Friedman test followed by Dunn's
702 multiple comparison.
703
704 **Figure 5: Pneumococcal carriage triggers monocyte to macrophage differentiation. a)** Levels of
705 monocytes and AMs in the BAL of carriage negative (n=8, black dots) and carriage positive individuals
706 (n=9, red dots), expressed as percentage of $CD45^{+}$ cells. Significant comparison of AM levels and AM:
707 Monocytes ratio between the two study groups, * p=0.046 by Mann-Whitney test. Medians and
708 interquartile ranges are shown per cell population. **b**) Monocytes and neutrophils analysed based on
709 their CD14, CD16 expression. For monocytes CD16 expressional levels divided them to two subsets,
710 $CD14^{hi}CD16^{lo}$ and $CD14^{hi}CD16^{hi.}$ Medians and interquartile ranges are shown per cell population. c)
711 Top pathways after gene set enrichment analysis for pathways and function applied on 2logFC (n= 5
712 subjects per group). NES presented in gradient colour. Red shades indicate pathways over-presented,
713 whereas blue shades pathways under-presented in the carriage positive group. 100% Significance
714 scored the pathways with **p <0.001, 80% pathways with *p<0.05 and 20% pathways with p>0.05. **d-**
715 **e)** Correlations between alveolar macrophage OPA and 2log CPM of *TBX21* and *NT5E*, respectively.
716

717 **Figure 6: Evidences of pneumococcal presence in the lung of nasopharyngeal *Spn* colonised**
718 **individuals. a)** Positive correlation between the nasal pneumococcal density, expressed as the Area
719 Under the Curve (logAUC) and the copies of pneumococcal DNA (*Spn6B*) detected in the BAL fluid of
720 *Spn* colonised individuals. r= 0.71, *p=0.02 by Pearson correlation test. **b)** Duration and density of
721 nasal colonisation per individual with detected *Spn6B* DNA in the BAL fluid (9 in 22 *Spn* colonised). The
722 end of each coloured line indicates the time point that the subject has cleared colonisation, assessed

723 by classical microbiology. **c)** Positive correlation between the nasal pneumococcal density (logAUC)
724 and sorted AMs opsonophagocytic activity (n=13). Pearson correlation, r= 0.06, *p=0.02. **d-e)**
725 Representative images taken by confocal microscope showing: **d)** pneumococci around AMs and **e)**
726 internalised pneumococci by AMs derived from Spn colonised individuals. CD14-red, nucleus-
727 DAPI/blue and Spn6 capsule-green. Scale bar= 2µm.
728
729 **Figure 7: Schematic overview**
730
731
732
733 **Figure S1:** Gating strategy of CD4+ T cells for transcriptions factors - Tbet, Gata-3 and Foxp3 -
734 expression for one representative volunteer.
735
736 **Figure S2:** Gating strategy of cytokine (INF-γ, TNF-a and IL-17A) producing cells analysis at baseline
737 and post-stimulation with HI-Spn6B. Gates from one representative volunteer are shown.
738
739 **Figure S3:** Gating strategy of TNF-a expression intracellularly by AMs post treatment with IFN-g and
740 stimulation with HI-Spn6B. Gates from one representative volunteer are shown.
741
742 **Figure S4:** Gating strategy of monocytes analysis for one representative volunteer.
743
744

Cytokine	Median concentration Carriage neg.	Median concentration Carriage pos.	p-value	adjusted p-value
IL2	0.17	0.17	9.36E-01	9.36E-01
IL17	0.30	0.30	1.42E-01	6.34E-01
TNFα	0.42	0.42	7.41E-01	9.31E-01
FGF Basic	0.65	0.65	1.83E-01	6.34E-01
GM-CSF	0.49	0.96	3.41E-02	4.84E-01
EGF	1.01	1.01	6.19E-01	9.12E-01
IL 10	0.92	1.11	4.43E-01	8.31E-01
IL 1β	1.09	1.09	2.90E-01	7.25E-01
IL 4	1.25	1.24	6.17E-01	9.12E-01
Eotaxin	1.19	1.33	9.14E-01	9.36E-01

RANTES	1.79	1.79	9.03E-01	9.36E-01
IL 5	2.30	2.78	3.61E-01	8.31E-01
IFN-γ	1.89	3.20	4.84E-02	4.84E-01
IFNα	2.96	3.61	4.43E-02	4.84E-01
MIG	2.07	7.37	1.11E-01	6.34E-01
IL 13	4.87	6.03	1.00E-01	6.34E-01
IL 12	8.13	7.07	8.84E-01	9.36E-01
MIP 1α	9.35	9.57	4.29E-01	8.31E-01
MIP 1β	11.00	11.42	5.03E-01	8.87E-01
IL 15	16.56	11.29	2.32E-01	6.34E-01
IL 6	13.49	16.22	2.03E-01	6.34E-01
IL 2R	17.62	22.65	4.06E-01	8.31E-01
IL 7	17.58	25.34	1.77E-01	6.34E-01
IP 10	23.07	29.58	2.12E-01	6.34E-01
G-CSF	33.03	43.81	7.33E-01	9.31E-01
MCP 1	51.34	48.13	8.95E-01	9.36E-01
VEGF	56.40	61.40	6.38E-01	9.12E-01
HGF	79.20	73.13	8.00E-01	9.36E-01
IL 8	61.92	90.55	5.38E-01	8.97E-01
IL 1RA	959.97	775.27	7.45E-01	9.31E-01

Table S1. Levels of 30 cytokines and chemokines measured the in the BAL fluid of carriage negative (n=20) and carriage positive (n=22) volunteers, who underwent research bronchoscopy up to 50 days post the pneumococcal inoculation. Levels are expressed as pg/ml and are ordered from low to high values. Median per group, p-values by Mann-Whitney test and p-values corrected by multiple-comparison testing (Benjamini-Hochberg) are displayed.

Gene	**log2FoldChange**	**p-value**	**adjusted p-value**
C1QA	-1.73	1.17E-03	4.25E-01
CD14	-1.86	3.95E-03	5.00E-01
CSF1R	-1.84	7.82E-03	5.00E-01
IRF4	1.77	8.43E-03	5.00E-01
C1QB	-1.66	9.23E-03	5.00E-01
CXCL11	1.96	1.05E-02	5.00E-01
GPI	-1.27	1.13E-02	5.00E-01
NT5E	1.38	1.81E-02	5.00E-01
CCND3	-1.45	1.83E-02	5.00E-01

CLEC7A	2.37	2.10E-02	5.00E-01
CEACAM6	1.29	2.16E-02	5.00E-01
LY96	2.19	2.24E-02	5.00E-01
TAPBP	-1.34	2.41E-02	5.00E-01
TNFSF4	1.32	2.61E-02	5.00E-01
HLA-DRB3	-3.36	2.82E-02	5.00E-01
ITGAX	-1.83	2.85E-02	5.00E-01
IL13	1.18	2.98E-02	5.00E-01
FCGRT	-1.32	3.18E-02	5.00E-01
CMKLR1	-1.55	3.28E-02	5.00E-01
TNFSF13B	1.78	3.37E-02	5.00E-01
CD164	2.01	3.48E-02	5.00E-01
S100A8	-1.46	3.52E-02	5.00E-01
CXCL2	2.08	3.62E-02	5.00E-01
PYCARD	-1.02	3.62E-02	5.00E-01
TBX21	1.42	3.67E-02	5.00E-01
TAGAP	1.08	3.72E-02	5.00E-01
KLRC4	1.24	3.78E-02	5.00E-01
CCRL1	1.27	3.85E-02	5.00E-01
GAPDH	-1.42	4.05E-02	5.08E-01
IL10RA	-1.14	4.48E-02	5.43E-01
TLR8	1.56	4.72E-02	5.45E-01
KIR3DL2	1.25	4.84E-02	5.45E-01
ITGB2	-1.41	4.94E-02	5.45E-01

754 **Table S2.** List of differentially expressed genes (DEG with $p < 0.05$) in sorted AMs on the day
755 of the bronchoscopy (36 to 115 days post intranasal inoculation), compared *Spn* colonised
756 (n=5) to non-colonised (n=5) individuals. Log2fold change (carriage positive over carriage
757 negative), p-values by Mann-Whitney test and corrected p-values by using Benjamini-
758 Hochberg procedure are displayed.
759

760

Variable1	**Variable2**	**p value**	**Rho**
KLRD1	OPA	0.007	0.818
SLAMF1	OPA	0.008	0.806
IL13RA1	OPA	0.011	0.760
CCL15	OPA	0.016	0.758
KIR3DL1	OPA	0.018	0.745
KLRAP1	OPA	0.018	0.745

IL16	OPA	0.021	0.733
PRDM1	OPA	0.024	0.721
CCR10	OPA	0.028	0.709
LAG3	OPA	0.028	0.709
TRAF4	OPA	0.028	0.709
IRF8	OPA	0.030	0.681
EDNRB	OPA	0.035	0.669
KLRK1	OPA	0.035	0.669
IL6R	OPA	0.035	0.685
NT5E	OPA	0.035	0.685
ZAP70	OPA	0.035	0.685
DPP4	OPA	0.039	0.657
CD7	OPA	0.039	0.673
CEACAM6	OPA	0.039	0.673
FCER1A	OPA	0.039	0.673
LILRA4	OPA	0.039	0.673
IL12A	OPA	0.042	0.650
BCL2	OPA	0.044	0.661
MASP2	OPA	0.044	0.661
TBX21	OPA	0.044	0.661
TNFRSF9	OPA	0.044	0.661
HLA.DOB	OPA	0.049	0.648
IRF5	OPA	0.049	0.648
LILRA3	OPA	0.049	0.648
LILRA5	OPA	0.049	0.648
SELL	OPA	0.049	0.648
TLR8	OPA	0.049	0.648
TNFRSF14	OPA	0.049	0.648

761

762 **Table S3.** List of genes for which expression significantly positively correlates with AM
763 opsonophagocytic activity.

Methods of spn6B DNA detection in BAL and NP	**Carriage pos.**	**Carriage neg.**
Spn6B detected in the BAL by qPCR	9/22 (41%)	0/21 (0%)
Live Spn6B detected in BAL by culturing	2/16 (12.5%)	0/10 (0%)
Live Spn6B detected in NP swabs by culturing	0/6 (0%)	0/6 (0%)

764

765 **Table S4. Methods of Spn6B detection in lung and nose the day of research bronchoscopy.**

766 Spn6B DNA was detected in 41% of carriage positive volunteers (9 in 22 carriers) by qPCR targeting a
767 Spn6B specific capsular polysaccharide gene. Spn6B DNA was not detected in any (0/21) non-colonised
768 subjects. Nasopharyngeal (NP) samples were taken prior to the bronchoscopy from 12 participants.
769 No live SPN6B was detected in any NP sample after culturing, whereas in two *Spn*-colonised volunteers
770 SPN6B growth was observed by classical microbiology plating of BAL fluid.
771
772
773
774
775

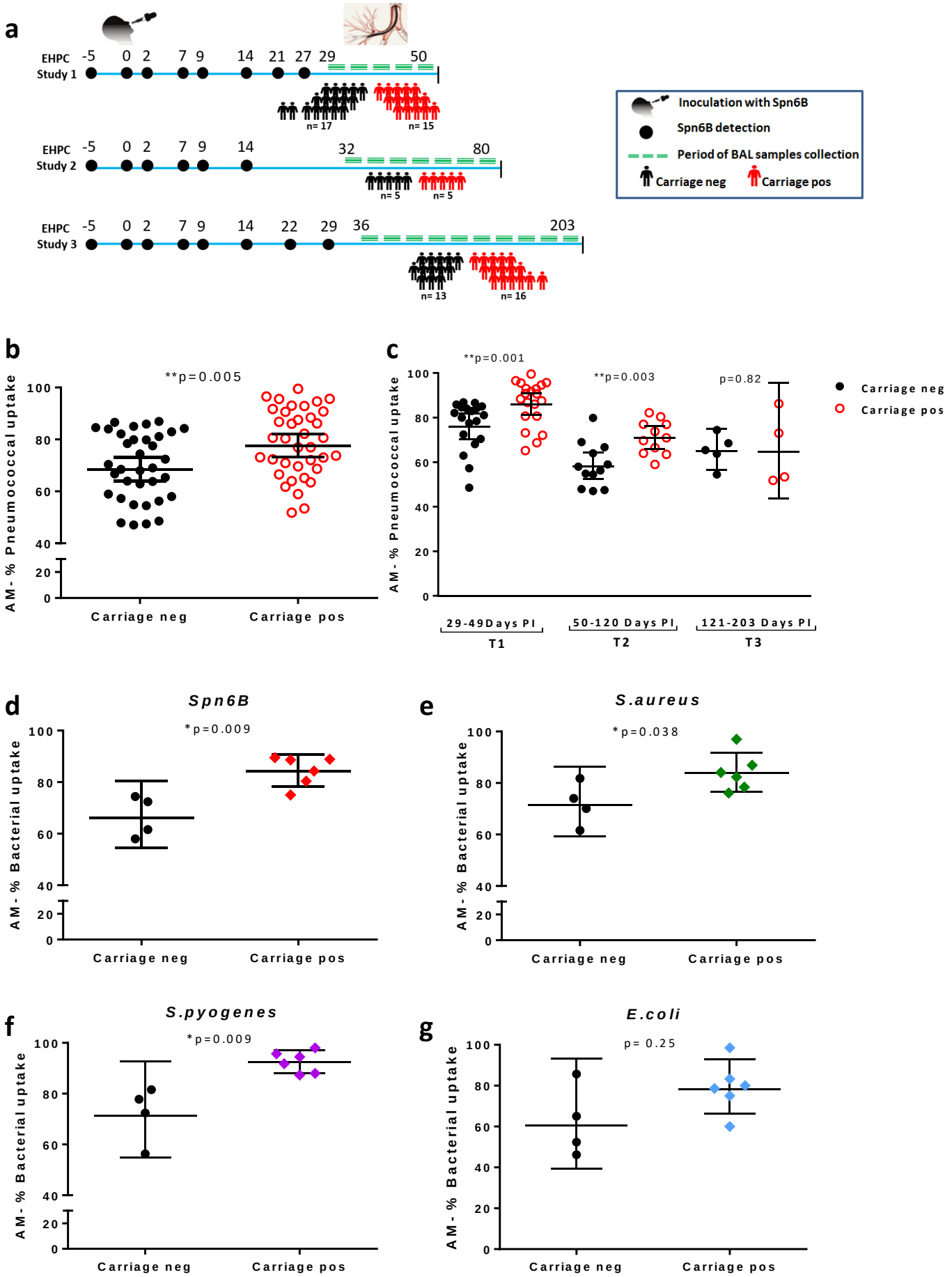
a
EHPC Study 1
-5 0 2 7 9 14 21 27 29 50
n= 17
n= 15
EHPC Study 2
-5 0 2 7 9 14 32 80
n= 5
n= 5
EHPC Study 3
-5 0 2 7 9 14 22 29 36 203
n= 13
n= 16
Inoculation with Spn6B
Spn6B detection
Period of BAL samples collection
Carriage neg
Carriage pos
b
AM - % Pneumococcal uptake
**p=0.005
Carriage neg
Carriage pos
c
AM - % Pneumococcal uptake
**p=0.001
**p=0.003
p=0.82
29-49Days PI
50-120 Days PI
121-203 Days PI
T1
T2
T3
Carriage neg
Carriage pos
d
Spn6B
AM - % Bacterial uptake
*p=0.009
Carriage neg
Carriage pos
e
S.aureus
AM - % Bacterial uptake
*p=0.038
Carriage neg
Carriage pos
f
S.pyogenes
AM - % Bacterial uptake
*p=0.009
Carriage neg
Carriage pos
g
E.coli
AM - % Bacterial uptake
p= 0.25
Carriage neg
Carriage pos

Figure 1

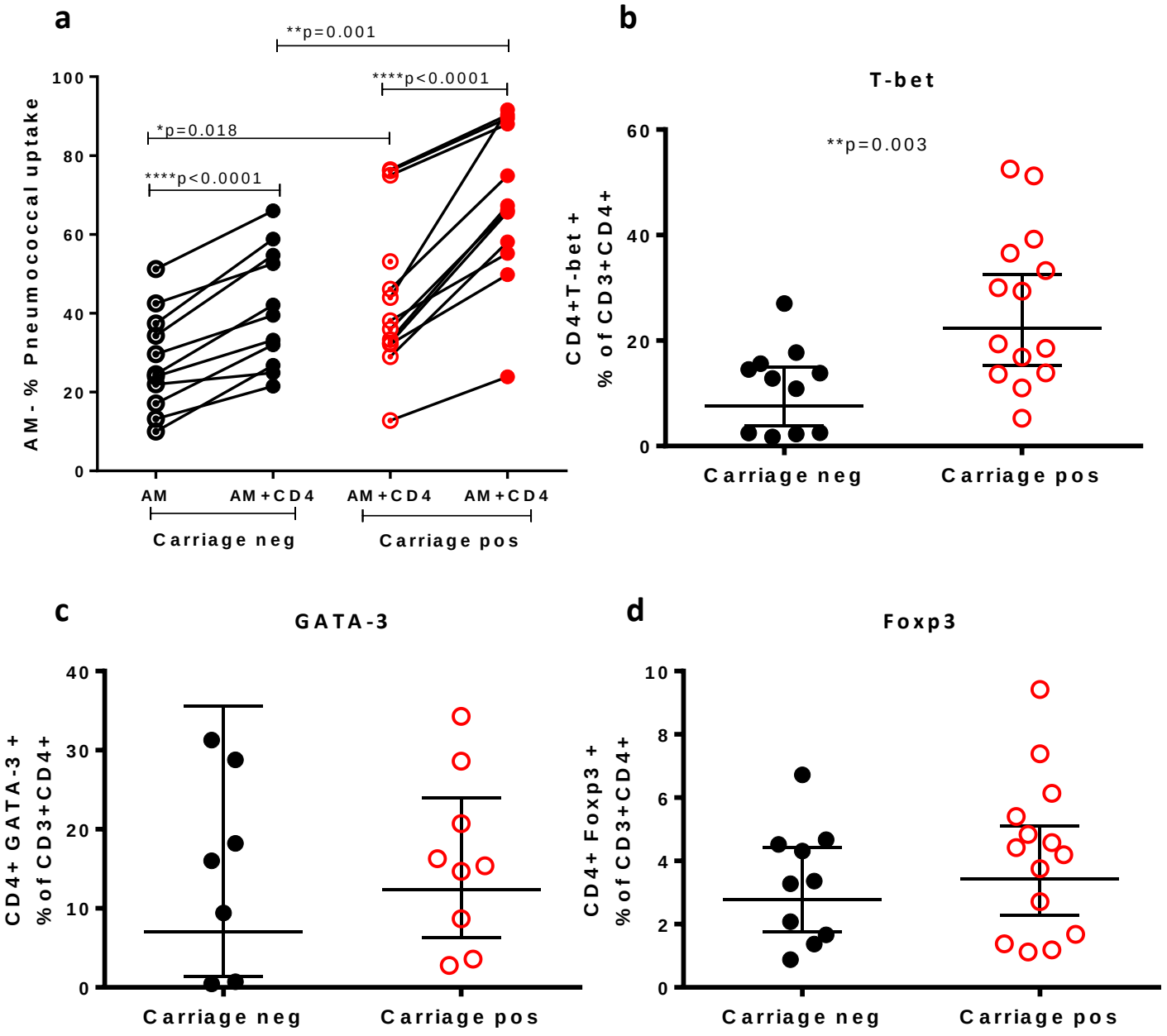
a
**p=0.001
****p<0.0001
*p=0.018
****p<0.0001
AM - % Pneumococcal uptake
100
80
60
40
20
0
AM
AM+CD4
AM+CD4
AM+CD4
Carriage neg
Carriage pos
b
T-bet
**p=0.003
CD4+T-bet+
% of CD3+CD4+
60
40
20
0
Carriage neg
Carriage pos
c
GATA-3
CD4+ GATA-3 +
% of CD3+CD4+
40
30
20
10
0
Carriage neg
Carriage pos
d
Foxp3
CD4+ Foxp3 +
% of CD3+CD4+
10
8
6
4
2
0
Carriage neg
Carriage pos

Figure 2

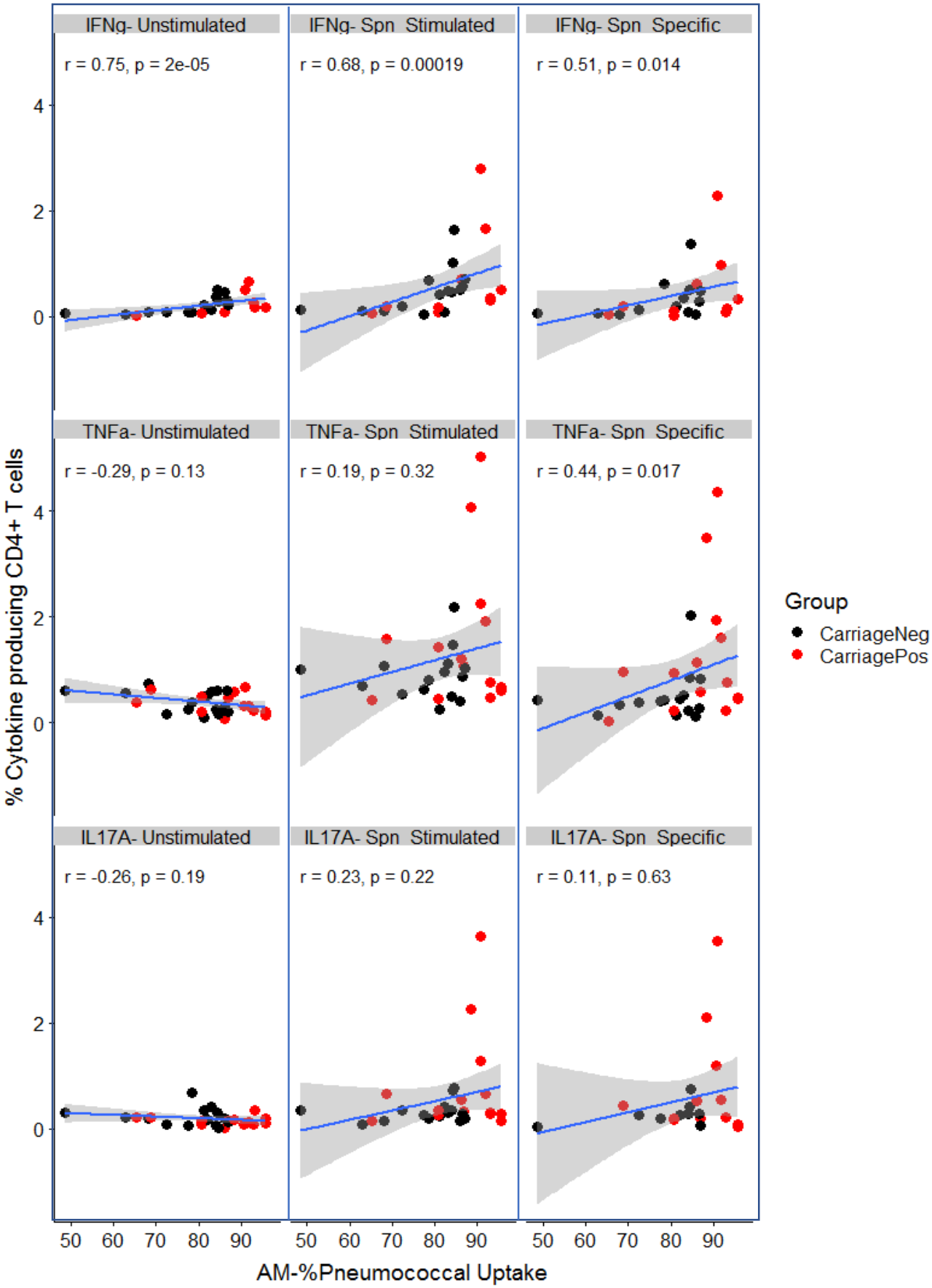
IFNg- Unstimulated
r = 0.75, p = 2e-05
IFNg- Spn Stimulated
r = 0.68, p = 0.00019
IFNg- Spn Specific
r = 0.51, p = 0.014
TNFa- Unstimulated
r = -0.29, p = 0.13
TNFa- Spn Stimulated
r = 0.19, p = 0.32
TNFa- Spn Specific
r = 0.44, p = 0.017
IL17A- Unstimulated
r = -0.26, p = 0.19
IL17A- Spn Stimulated
r = 0.23, p = 0.22
IL17A- Spn Specific
r = 0.11, p = 0.63
% Cytokine producing CD4+ T cells
AM-%Pneumococcal Uptake
Group
CarriageNeg
CarriagePos

Figure 3

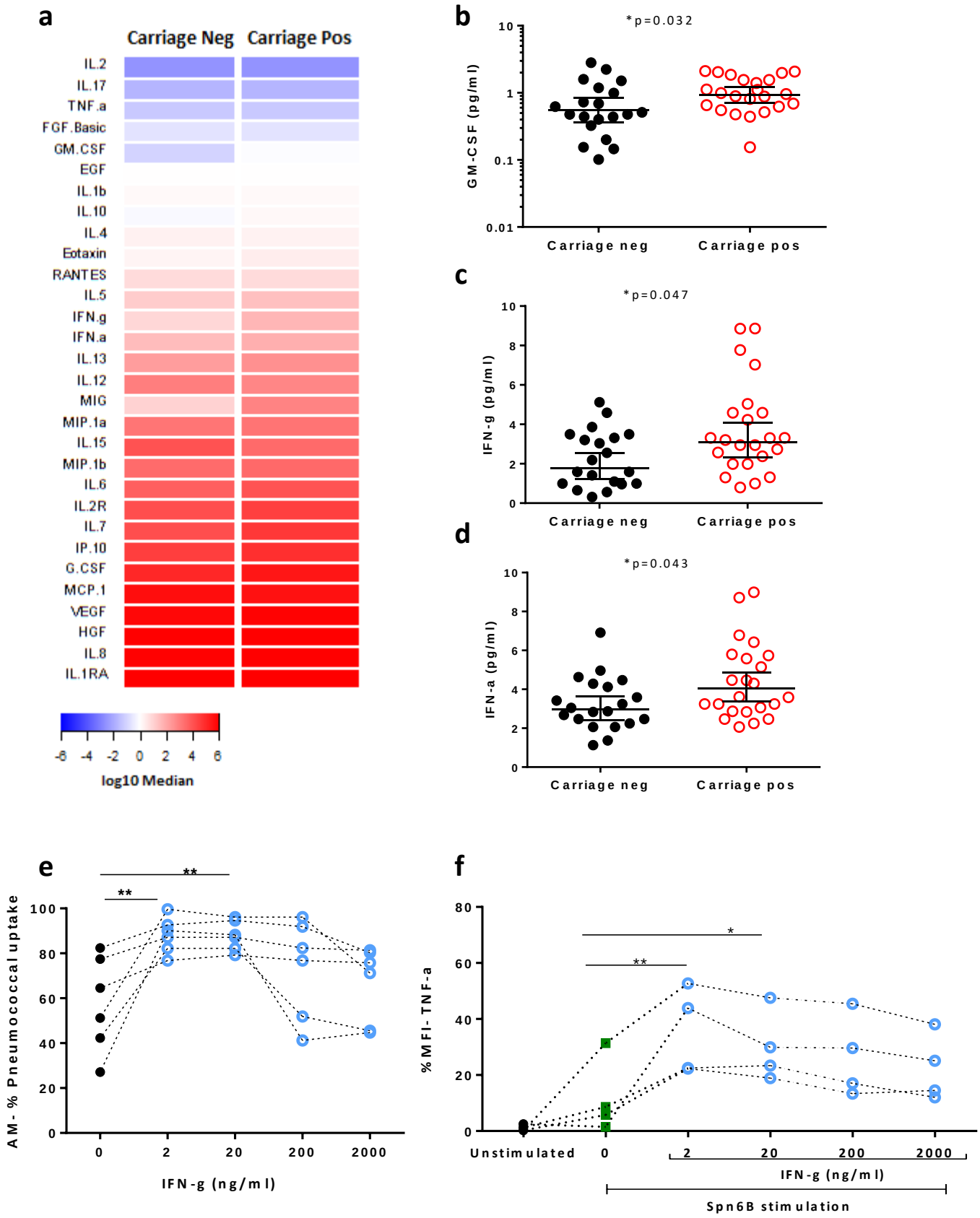
a
Carriage Neg
Carriage Pos
IL.2
IL.17
TNF.a
FGF.Basic
GM.CSF
EGF
IL.1b
IL.10
IL.4
Eotaxin
RANTES
IL.5
IFN.g
IFN.a
IL.13
IL.12
MIG
MIP.1a
IL.15
MIP.1b
IL.6
IL.2R
IL.7
IP.10
G.CSF
MCP.1
VEGF
HGF
IL.8
IL.1RA
-6 -4 -2 0 2 4 6
log10 Median
b
*p=0.032
GM-CSF (pg/ml)
10
1
0.1
0.01
Carriage neg
Carriage pos
c
*p=0.047
IFN-g (pg/ml)
10
8
6
4
2
0
Carriage neg
Carriage pos
d
*p=0.043
IFN-a (pg/ml)
10
8
6
4
2
0
Carriage neg
Carriage pos
e
**
**
AM- % Pneumococcal uptake
100
80
60
40
20
0
0
2
20
200
2000
IFN-g (ng/ml)
f
*
**
% MFI- TNF-a
80
60
40
20
0
Unstimulated
0
2
20
200
2000
IFN-g (ng/ml)
Spn6B stimulation

Figure 4

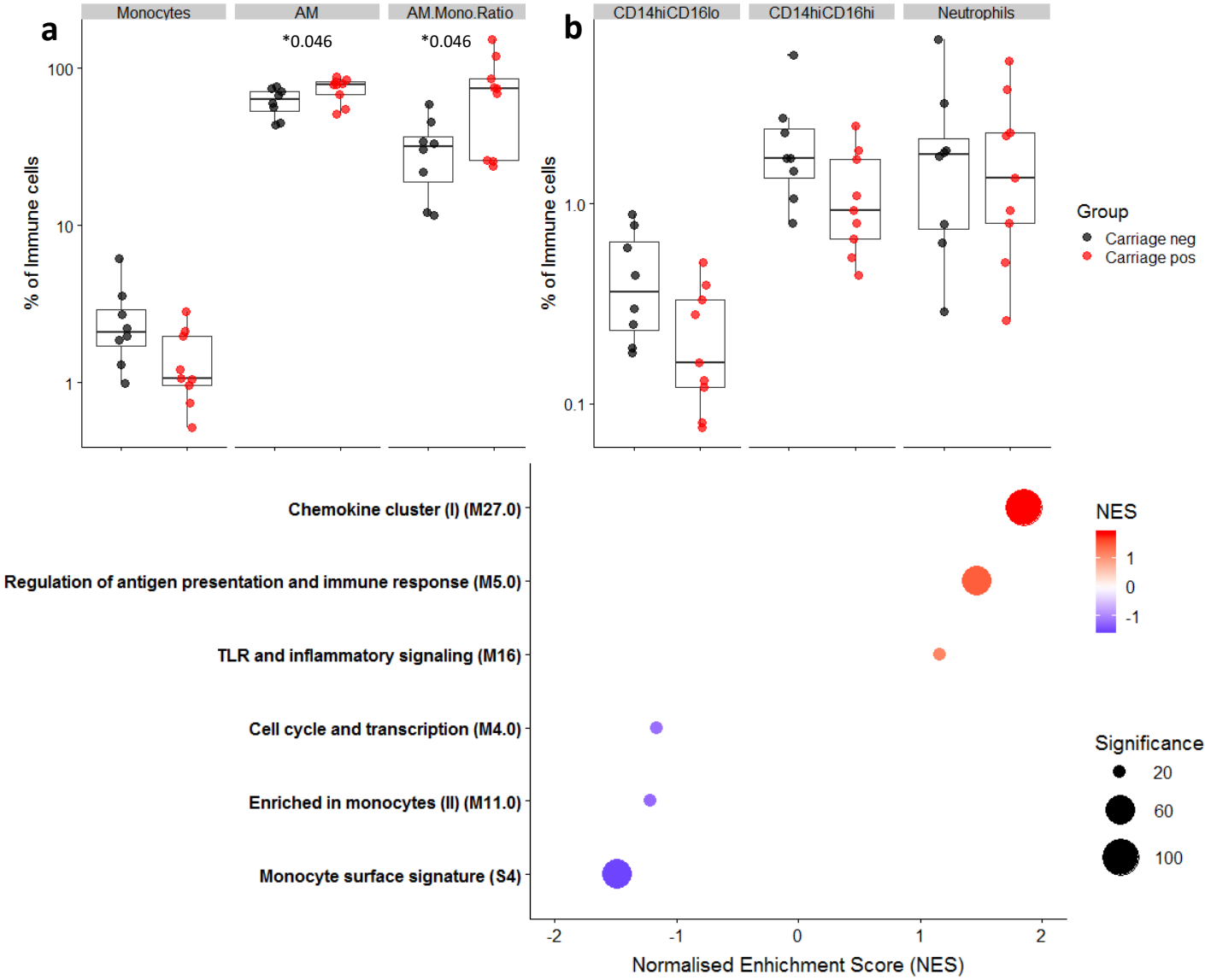
a
Monocytes
AM
AM.Mono.Ratio
*0.046
*0.046
% of Immune cells
100
10
1
b
CD14hiCD16lo
CD14hiCD16hi
Neutrophils
% of Immune cells
1.0
0.1
Group
Carriage neg
Carriage pos
Chemokine cluster (I) (M27.0)
Regulation of antigen presentation and immune response (M5.0)
TLR and inflammatory signaling (M16)
Cell cycle and transcription (M4.0)
Enriched in monocytes (II) (M11.0)
Monocyte surface signature (S4)
-2
-1
0
1
2
Normalised Enhichment Score (NES)
NES
1
0
-1
Significance
20
60
100

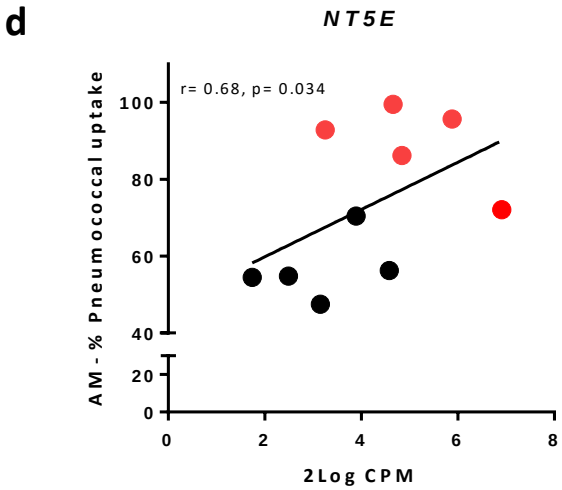
d
NT5E
r= 0.68, p= 0.034
AM - % Pneumococcal uptake
100
80
60
40
20
0
0
2
4
6
8
2Log CPM

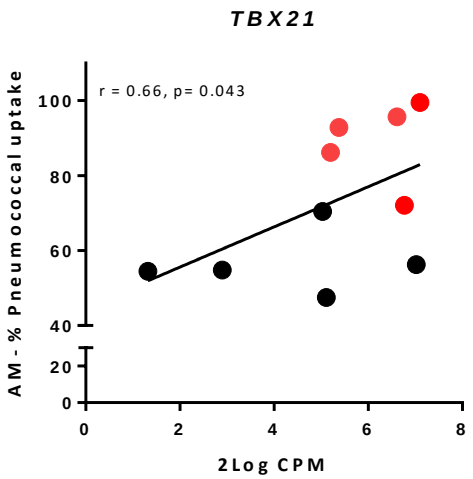
e
TBX21
r = 0.66, p= 0.043
AM - % Pneumococcal uptake
100
80
60
40
20
0
0
2
4
6
8
2Log CPM

Figure 5

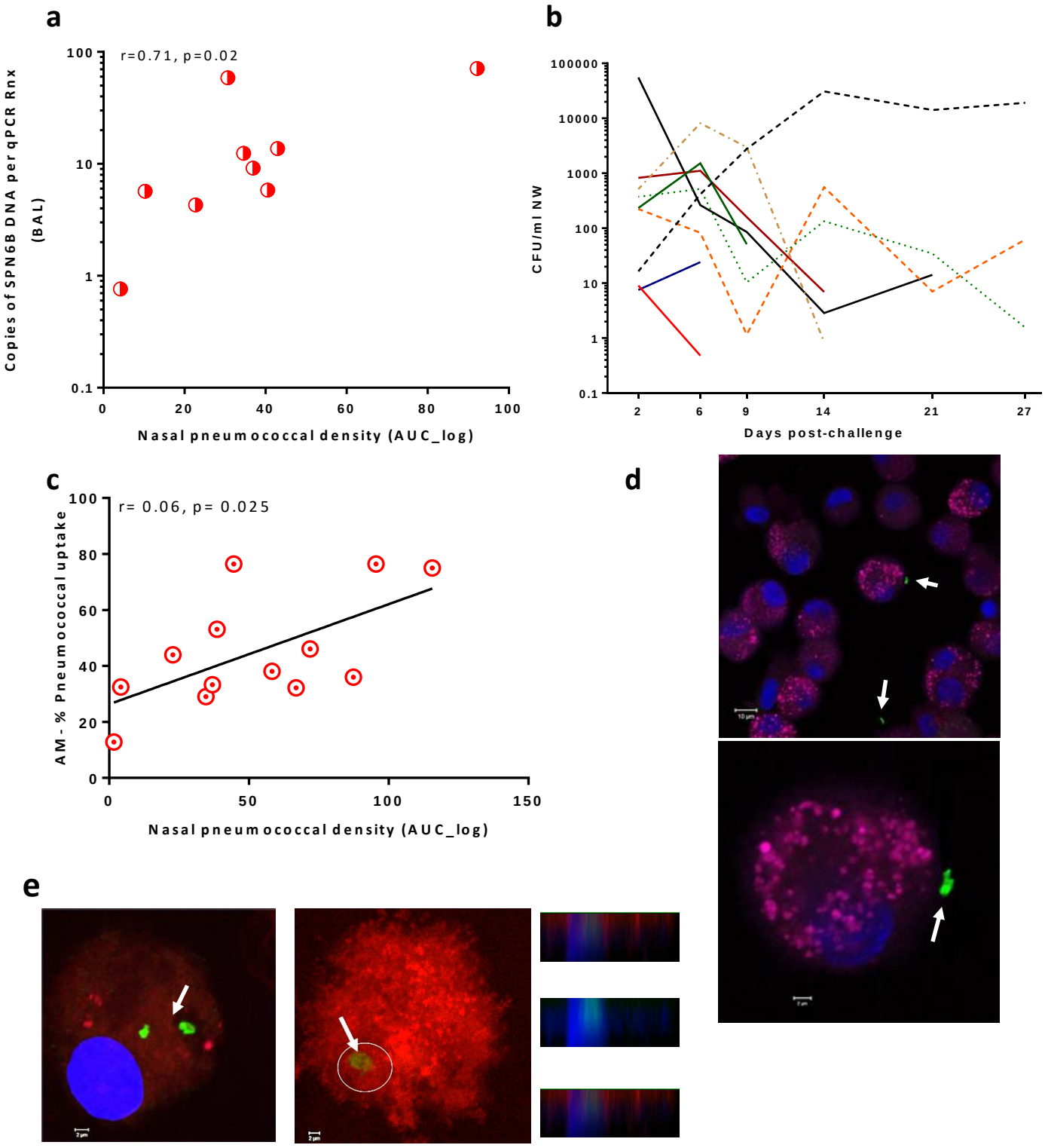
a
r=0.71, p=0.02
Copies of SPN6B DNA per qPCR Rnx (BAL)
Nasal pneumococcal density (AUC_log)
b
CFU/ml NW
Days post-challenge
c
r= 0.06, p= 0.025
AM - % Pneumococcal uptake
Nasal pneumococcal density (AUC_log)
d
e

Figure 6

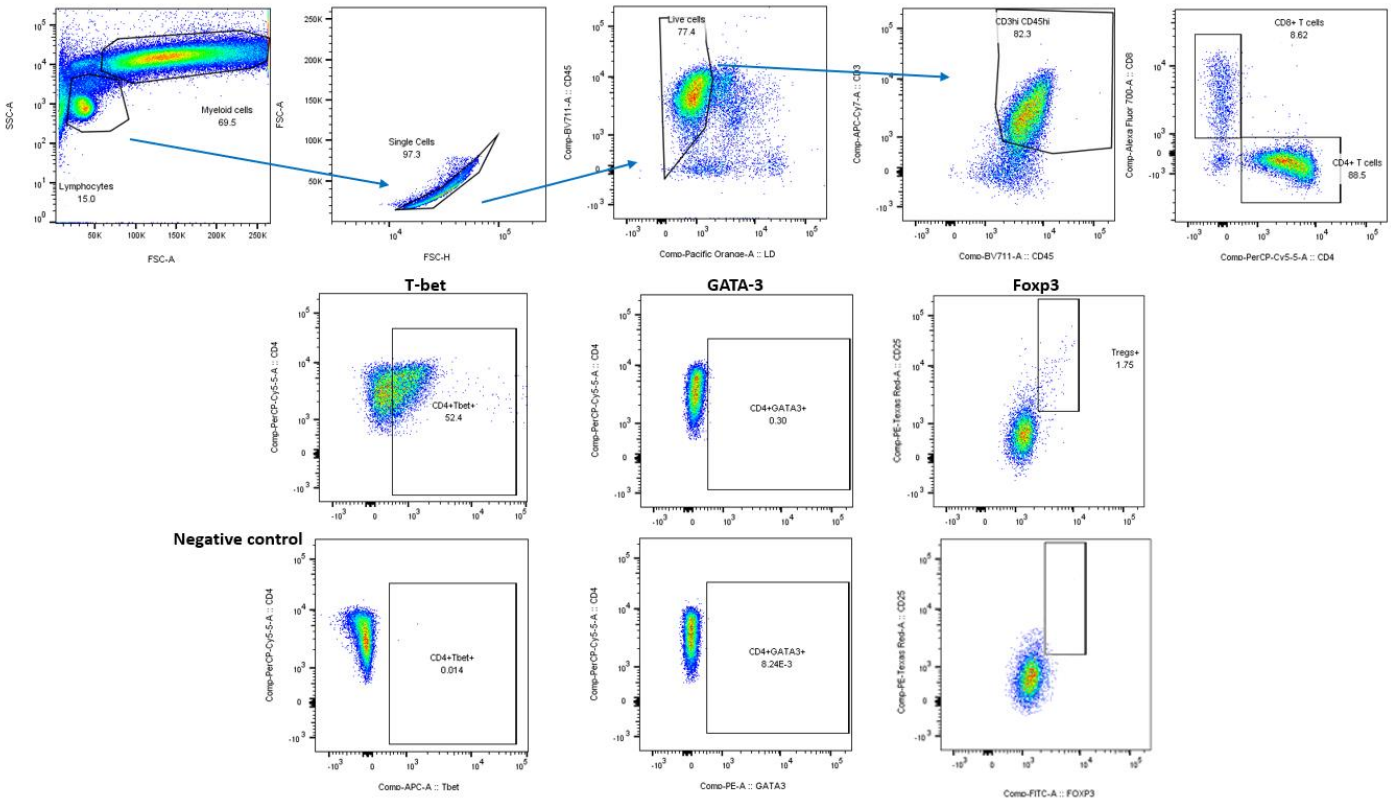

Supplementary figure 1

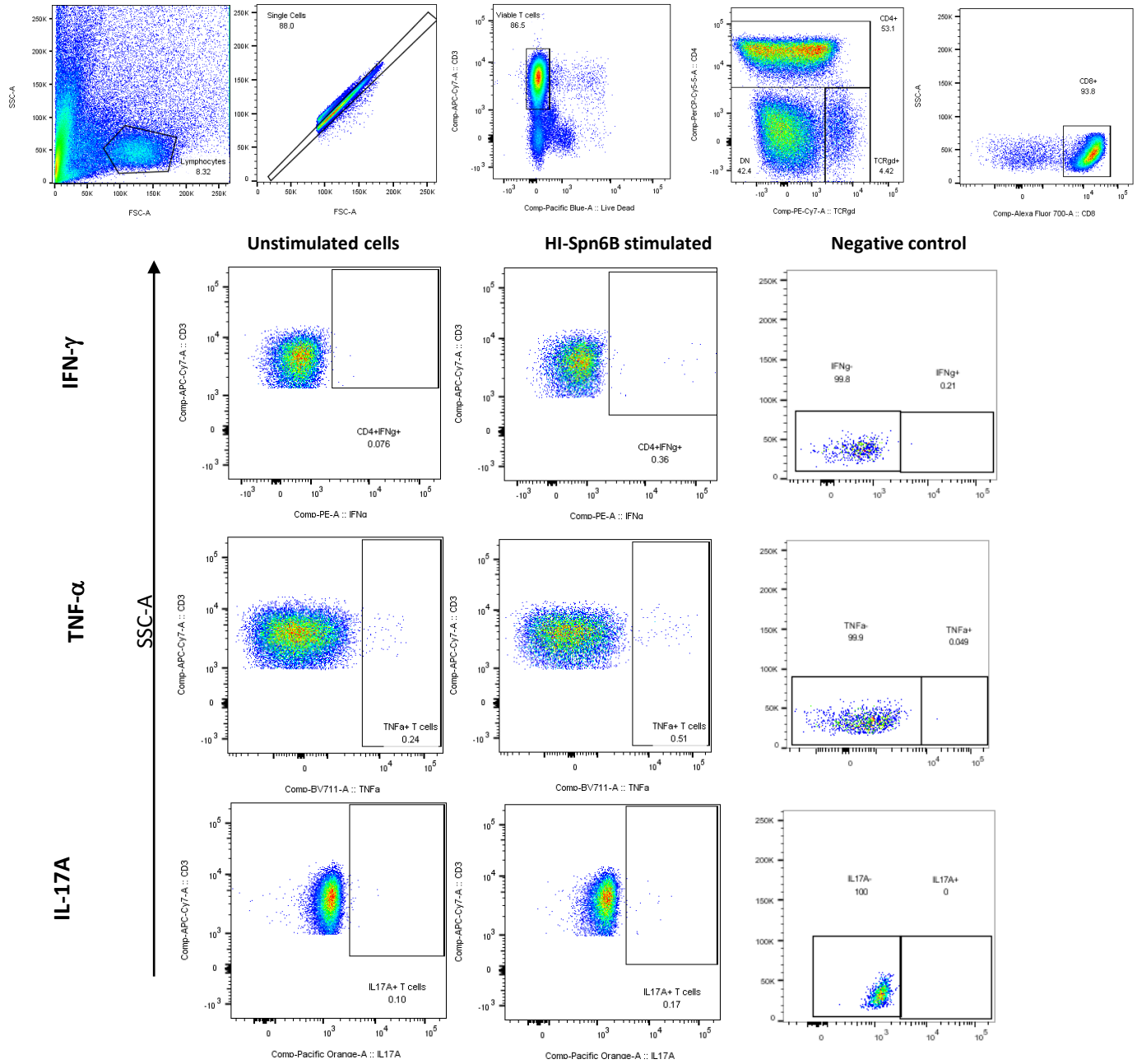

Supplementary figure 2

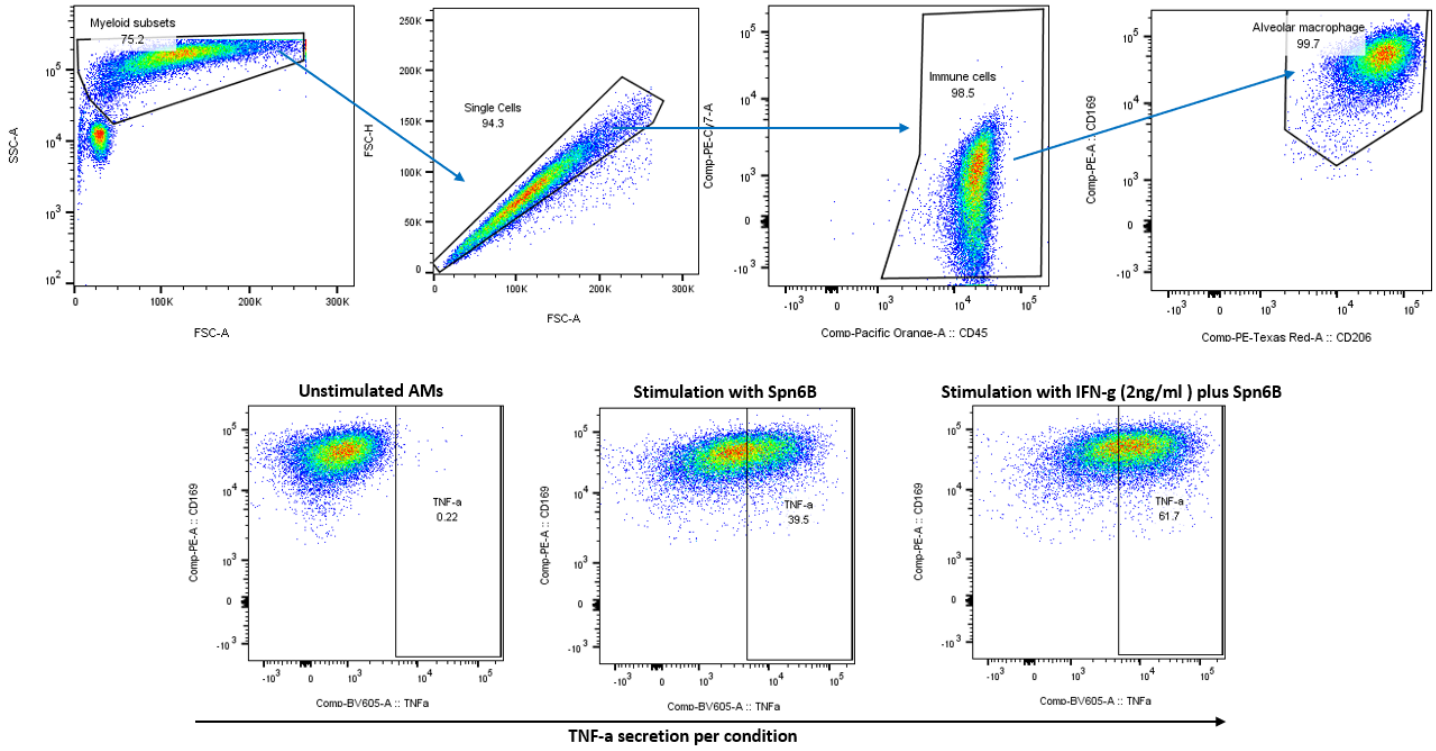

Supplementary figure 3

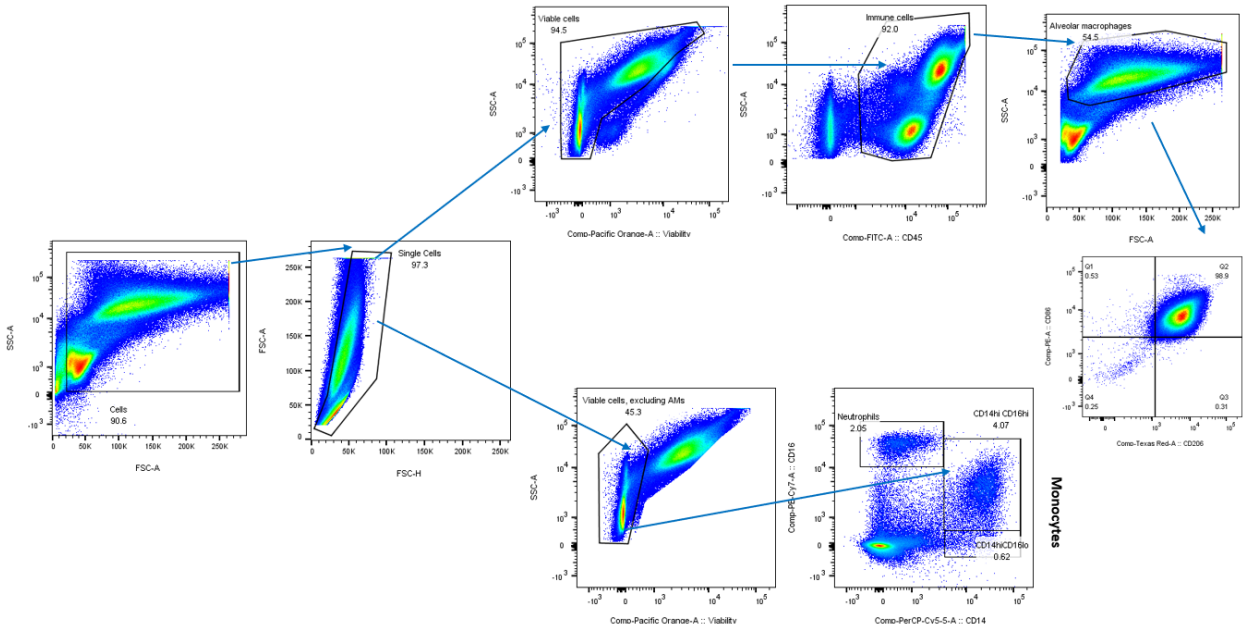

Supplementary Figure 4

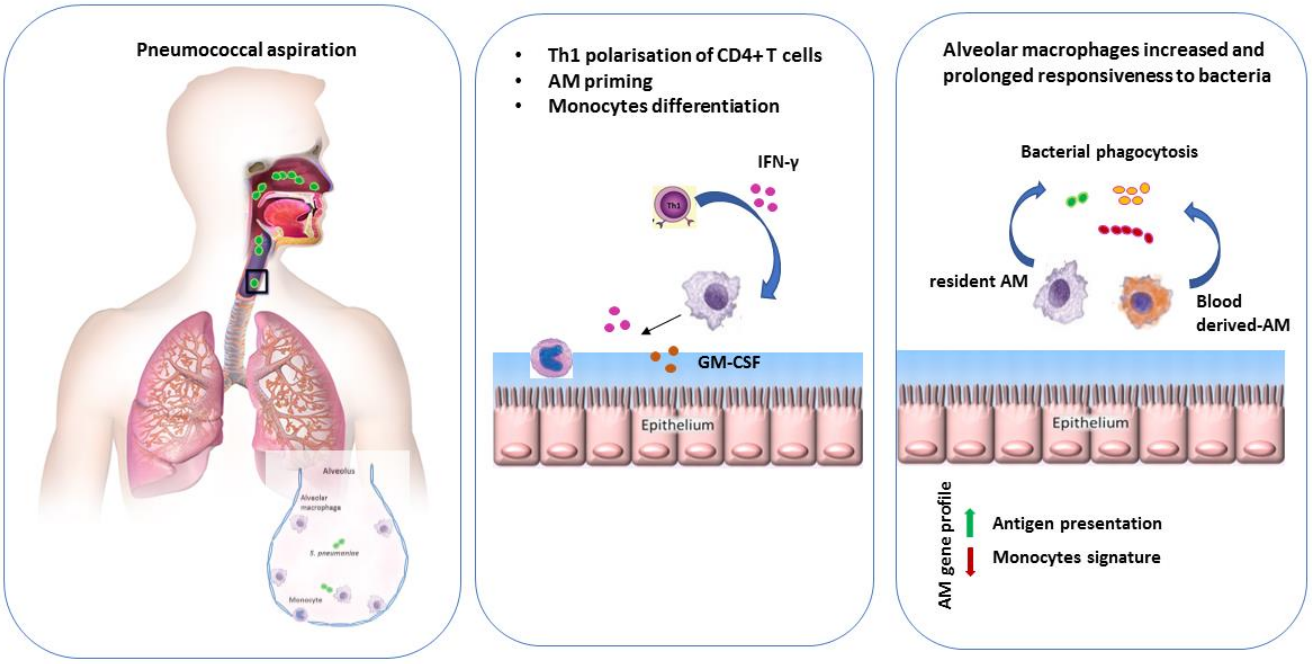

Schematic overview- Draft version